PL-TR-94-2119

MULTIPLE INSTRUMENT STUDIES OF CHEMICAL RELEASES AND HEATING AT ARECIBO

Robert C. Livingston
Craig J. Heinselman
James F. Vickrey
Roland T. Tsunoda

SRI International
333 Ravenswood Avenue
Menlo Park, CA 94025

March 1994

Final Report
July 1990 - September 1993

PHILLIPS LABORATORY
Directorate of Geophysics
AIR FORCE MATERIEL COMMAND
HANSCOM FORCE BASE, MASS 01731-3010

"This technical report has been reviewed and is approved for publication"

EDWARD J. WEBER
Contract Manager

EDWARD J. BERGHORN
Branch Chief

WILLIAM K. VICKERY
Division Director

This document has been reviewed by the ESD Public Affairs Office (PA) and is releasable to the National Technical Information Service (NTIS).

Qualified requestors may obtain additional copies from the Defense Technical Information Center. All others should apply to the National Technical Information Service.

If your address has changed, or if you wish to be removed from the mailing list, or if the addressee is no longer employed by your organization, please notify PL/TSI, Hanscom AFB, MA 01731-5000. This will assist us in maintaining a current mailing list.

Do not return copies of this report unless contractual obligations or notices on a specific document requires that it be returned.

REPORT DOCUMENTATION PAGE

Form Approved
OMB No. 0704-0188

1. AGENCY USE ONLY (Leave Blank)	2. REPORT DATE	3. REPORT TYPE AND DATES COVERED
	March 1994	Final July, 1990 - September 1993

4. TITLE AND SUBTITLE

Multiple Instrument Studies of Chemical Releases and Heating at Arecibo

5. FUNDING NUMBERS

PE: 61102F
PR 2310 TA G9 WU AJ

Contract F19628-90-K-0036

6. AUTHORS

R.C. Livingston, C.J. Heinselman, J.F. Vickrey, R.T. Tsunoda

7. PERFORMING ORGANIZATION NAME(S) AND ADDRESS(ES)

SRI International
333 Ravenswood Avenue
Menlo Park, CA 94025-3493

8. PERFORMING ORGANIZATION REPORT NUMBER

9. SPONSORING/MONITORING AGENCY NAME(S) AND ADDRESS(ES

Phillips Laboratory
29 Randolf Road
Hanscom AFB, MA 01731-3010
Contract Manager: Edward Weber/GPIA

10. SPONSORING/MONITORING AGENCY REPORT NUMBER

PL-TR-94-2119

11. SUPPLEMENTARY NOTES

12a. DISTRIBUTION/AVAILABILITY STATEMENT

Approved for public release; distribution unlimited

12b. DISTRIBUTION CODE

13. ABSTRACT *(Maximum 200 words)*

The Combined Releases and Radiation Effects Satellite (CRRES) Puerto Rico experiments carried out during June and July 1992, provided and opportunity to observe the dynamics and evolution of high-altitude chemical releases at middle latitudes. Among the experiments that were conducted for the program, three large barium payloads were released into the dawn F region -- two into the natural ionosphere and one into an ionosphere modified by HF heating. Extended periods of HF modification prior to the rocket launches also provided an opportunity to study heating effects, per se. This report reviews some preliminary results from three participating instruments: (1) ion-line mapping made by the Arecibo incoherent scatter radar, (2) HF backscatter characterization and tracking of the barium cloud, and (3) transionospheric propagation diagnosis of large and medium scale structure produced by heating and the barium releases. The data that are reviewed are primarily observational and are presented with a minimum of physical interpretation. Recommendations are made for further analysis of much of the data.

14. SUBJECT TERMS

Radiowave Scintillation, Ionospheric Modification, Barium Releases

High frequency Backscatter, Plasma Clouds, Ionospheric Plasmas

15. NUMBER OF PAGES

44

16. PRICE CODE

17. SECURITY CLASSIFICATION OF REPORT	18. SECURITY CLASSIFICATION OF THIS PAGE	19. SECURITY CLASSIFICATION OF ABSTRACT	20. LIMITATION OF ABSTRACT
Unclassified	Unclassified	Unclassified	SAR

CLASSIFIED BY:
N/A since Unclassified

DECLASSIFY ON:
N/A since Unclassified

CONTENTS

LIST OF ILLUSTRATIONS

LIST OF ILLUSTRATIONS (concluded)

LIST OF ABBREVIATIONS

ACF	autocorrelation function
AIO	Airborne Ionospheric Observatory (Phillips Laboratory)
CRRES	Combined Release and Radiation Effects Satellite
CW	continuous wave
FAR	frequency agile radar
ISR	incoherent scatter radar
PL	Phillips Laboratory
PRF	pulse repetition frequency
RF	radio frequency
SNR	signal-to-noise ratio
UT	Universal time

ABSTRACT

The Combined Release and Radiation Effects Satellite (CRRES) Puerto Rico experiments carried out during June and July 1992, provided an opportunity to observe the dynamics and evolution of high-altitude chemical releases at middle latitudes. Among the experiments that were conducted for the program, three large barium payloads were released into the dawn F region—two into the natural ionosphere and one into an ionosphere modified by HF heating. Extended periods of HF modification prior to the rocket launches also provided an opportunity to study heating effects, per se. This report reviews some preliminary results from three participating instruments:

- ion-line mapping made by the Arecibo incoherent scatter radar
- HF backscatter characterization and tracking of the barium cloud
- transionospheric propagation diagnosis of large and medium scale structure produced by heating and the barium releases.

The primary purpose of the incoherent scatter ion-line system at the Arecibo Observatory was to determine the suitability of ionospheric conditions for rocket launch, and to provide precise measurement of the barium cloud location and dynamics. Analysis of the incoherent scatter returns from the barium cloud has provided estimates of its temperature, composition, and motion. Velocity shears that may indicate rotation of the edges of the plasma cloud are observed.

An SRI HF radar was located near Arecibo in order to optimize the geometry for coherent backscatter returns from E-region images of barium cloud striations. Although the barium clouds were not observed to striate, overdense returns from the ion cloud were observed for an extended period after release. Processed in a way to obtain Doppler maps at various frequencies, the data show the evolution and motion of the ion cloud in time. Characteristics of the returns also indicate that there was no development of small scale structure within the cloud, although offset returns with high Doppler shifts are observed during the initial cloud growth.

The transionospheric propagation experiment measured plasma structure larger than about 100 m using a UHF satellite signal. It was operated from the Phillips Laboratory (PL) Airborne Ionospheric Observatory (AIO) aircraft, which flew a pattern that maintained the satellite signal path through the ion cloud. The cloud did not striate at the spatial scales that create scintillation, and intersections between the propagation path and the cloud are identifiable only as rapid changes in total electron content. Several hours of propagation data collected during ionospheric modification indicate the presence of very weak, hundreds-of-meters scale electron density perturbations within the heated volume.

The data reviewed are primarily observational and are presented with a minimum of physical interpretation. Recommendations are made for further analysis of much of the data.

1 INTRODUCTION

One objective of the CRRES rocket program was to study the striation of barium clouds and the corresponding formation of plasma images in the lower ionosphere. Plasma images form from electric fields that are mapped downward along the magnetic field from the cloud striations, and form most readily at the altitude where the Pedersen conductivity maximizes (typically ~130 km). The downward mapping of the electric field is scale-size dependent and is effective only for the larger stria in the cloud; this limits the images to spatial scale sizes of 1000 m or larger.

In order to adequately diagnose the barium cloud and lower ionosphere image region, the PL and SRI groups collaborated in data collection. Three instruments were used:

- real time ion line observations of the background ionosphere and the barium ion cloud made by the Arecibo 430 MHz incoherent scatter radar
- observations of the barium cloud and low-altitude image irregularities using a frequency agile radar (FAR) operating between 3 and 30 MHz
- measurements of the large and intermediate scale electron density structure produced by the ion cloud using UHF transionospheric satellite transmissions.

The original CRRES program included rocket launches from the south coast of Puerto Rico, and it was planned to directly diagnose the cloud image pattern using transionospheric phase scintillation. Releases launched from the north coast cannot be diagnosed in the same way since there is no land mass from which to observe the available satellite signal sources. Instead, scintillation measurements were made from aboard the Phillips Laboratory AIO aircraft flying in a pattern that made repeated cuts of the propagation path through the ion cloud. The amplitude and phase perturbations imparted to the signal can be used to characterize the ionization and any irregularity structure that develops within the cloud. The mobility of the AIO allowed it to maintain track of the barium cloud (or, in principle, the image region) as it drifted, but was also on station in a pattern designed to measure scintillation-producing structure within the HF heater beam prior to the rocket countdown.

The flight path of the AIO was directed from the Arecibo incoherent scatter radar, which tracked the cloud using a sequence of azimuth sector scans. The radar also monitored pre-launch conditions in order to ensure that the cloud would drift south or southwestward toward, and not away from the radar. The radar data collected in ion line mode also provided for post-mission analysis of ionospheric conditions during heating and chemical launch.

The SRI frequency agile radar system was selected as a means to additionally characterize cloud striation images. It was located near the Arecibo Observatory, where the line of sight propagation is perpendicular to the magnetic field at the altitude of maximum image growth (about 130 km). It was planned that the FAR would observe coherent returns from any short scale irregularities that formed in conjunction with the large scale images. At later times,

when the ionosphere was sunlit, refractive bending would allow the HF radar to see coherent returns from structure within the cloud, per se. Finally, the HF radar can track the cloud by Doppler mapping its overdense return signal.

The two Phillips Laboratory CRRES rockets were launched on July 2 (AA-1) and July 4, 1992 (AA-7) into the natural ionosphere. These were followed by a third payload (AA-2) that was released on July 12, 1992 into an actively heated region. Each rocket released 48 kg of barium vapor at altitudes near 250 km. Little was known about the structuring characteristics of such large chemical releases in the morning twilight. Similarly sized releases during the DNA Secede II program were all made in the evening twilight, or mid-afternoon. For the Spruce event of that program, which was a 48-kg release at 187 km, peak electron densities exceeded 2×10^7 el/cm^3, and the cloud was strongly striated within about 10 minutes (see e.g., Tsunoda, 1972). In contrast, the similar afternoon event Quince release did not structure (St.-Germain *et al*, 1972).

For all three of the CRRES releases discussed here, there is no evidence of any systematic structuring of the cloud, either in the HF radar signatures or in the propagation scintillation data. This might be attributable to either the altitude of the releases, or the prevailing morning twilight conditions. Despite the lack of striations and images, the instruments have provided much data of interest.

2 INCOHERENT SCATTER RADAR MEASUREMENTS

The primary function of the Arecibo incoherent scatter radar (ISR) during the CRRES campaign was to diagnose heating effects, and the effects of heating a barium cloud, using the plasma line technique. During such plasma line observations, the radar resources are dedicated to particular signal processing procedures that preclude any routine ion line measurements. Unfortunately, only the ion line technique provides estimates of ionospheric drift and electron density that are crucial to the CRRES program. That information was necessary to determine the suitability of launch conditions and to track the barium cloud after release. Furthermore, without ion line observations there is no spectral capability from which to estimate the temperature, composition, or motion of the plasma within the cloud, all of which are important to the physical understanding of the cloud evolution.

The Arecibo plasma line observations use a binary-coded waveform that generates a spectrum of seven lines across a bandwidth of approximately 250 kHz. The waveform and its associated analysis technique as described by Sulzer (1986) is also well suited for ion line observations. By spacing the transmitted carriers at least twice the ion spectral bandwidth, multiple independent estimates of that spectrum can be obtained. Given adequately high electron density, this improves the statistical confidence of the estimate by a factor of seven for the seven-line code used at Arecibo for CRRES.

Although the Arecibo radar system cannot simultaneously process plasma and ion lines from the seven-line waveform, the received analog signals are available for outboard processing. Therefore, for CRRES, SRI provided a data system with adequate processing power to combine the spread-spectrum return and to process and display the ion line spectral data. The data acquisition portion of that system is the same as that used at the Sondre Strømfjørd, Greenland, and ALTAIR Radar, Kwajalein ISR facilities. It consists of an AT-type computer with an array processor and an associated timing/sampling unit that samples and spectrally processes baseband quadrature output signals from a radar receiver. The timing control unit also provides the timing synchronization with the radar transmitter system. The connections between the data collection system and the Arecibo radar system were minimal, and include

- receiver output signals at baseband
- a TTL-level control line synchronized with the transmitter radio frequency (RF) on
- a 10 MHz clock reference signal from the radar.

A computer-controlled switch was also installed to alternatively route data from two radar receivers into the data collection system in order to use the split antenna feed system at Arecibo.

The Arecibo receivers have an IF bandwidth of about 2 MHz; the returns are mixed to baseband within a pre-sampling bandwidth of 125 kHz, using a filter customized to the Sulzer (1986) waveform. Within the SRI processor, the in-phase and phase-quadrature components are processed in real time using a time-domain technique to compute the autocorrelation function (ACF). A running series of all the lag products for each seventh lag are computed and summed throughout each sampled time series; this process is equivalent to the frequency domain approach

for which the ion line spectra are shifted and added. Both techniques supply a series of ACFs in range, which are then integrated in time and/or space within the data collection computer.

The SRI data acquisition computer operated on an ethernet LAN with two other AT-type computers. One of these obtained antenna position and housekeeping data from the radar and archived the ion line ACF data to disk. The second computer was used almost exclusively for real time online displays, but it also implemented an algorithm for resolving vector velocities from multiple line of sight measurements. Available displays included gray-shade maps of ion density and maps of ionospheric drift vectors.

2.1 JULY 2 RELEASE

The first PL rocket (AA-1) payload was released at 0903:33 Universal time (UT) on July 2, 1992, at an altitude of 255 km. Figure 1 shows the accumulated plasma drift velocity in magnetic coordinates at 250 km altitude for that day, prior to launch, and on through the time that the cloud remained within the field of view of the radar. Before 0900 UT, the velocity was resolved from a running series line of sight Doppler offsets measured during 360° azimuth scans and indicates a mostly southwestward flow of approximately 50 m/s. This direction of flow was desirable in that it tended to drive the ion cloud toward the radar, extending the period over which it could be tracked.

Following the release of the barium cloud, a series of narrow azimuth scans were made by the radar in order to maintain track of the cloud during its westward drift: the cloud was conspicuous in seven scans, up until about 0940 UT. The electron density profiles from six of the scans are shown in Figure 2. The cloud drifted from directly north of the radar to an azimuth of about 285° by 0930 UT. Each frame in the figure compares the profile through the highest density portion of the cloud with that measured just after exiting the cloud. (These profiles cannot be viewed as defining the shape of the barium cloud, since azimuth scans at Arecibo are made at a fixed elevation angle—75° in this case.) We believe that the first cuts in the figure are through the true center of the cloud, but the cloud drops in altitude with time so the later profiles scan only the top of the cloud. Eventually, the cloud drops out of the radar field of view. Throughout the scans, the cloud remains as a distinct plasma enhancement as it drops in altitude.

The electron density profiles in Figure 2 are not temperature-corrected. For the initial scans, the ionosphere is still dark and the temperature correction is negligible. The peak density of the background layer, calibrated using the ionosonde at 0856 UT, is therefore accurate. However, temperature correction does start to become significant after sunrise, and may produce background electron densities that are twice that shown. The peak electron density in the cloud can be derived only from a detailed correction for temperature and composition. However, the maximum raw density within the cloud of approximately 6×10^5 electrons/ cm^{-3} observed a few minutes after launch is much less than that observed for the lower altitude SECEDE II releases.

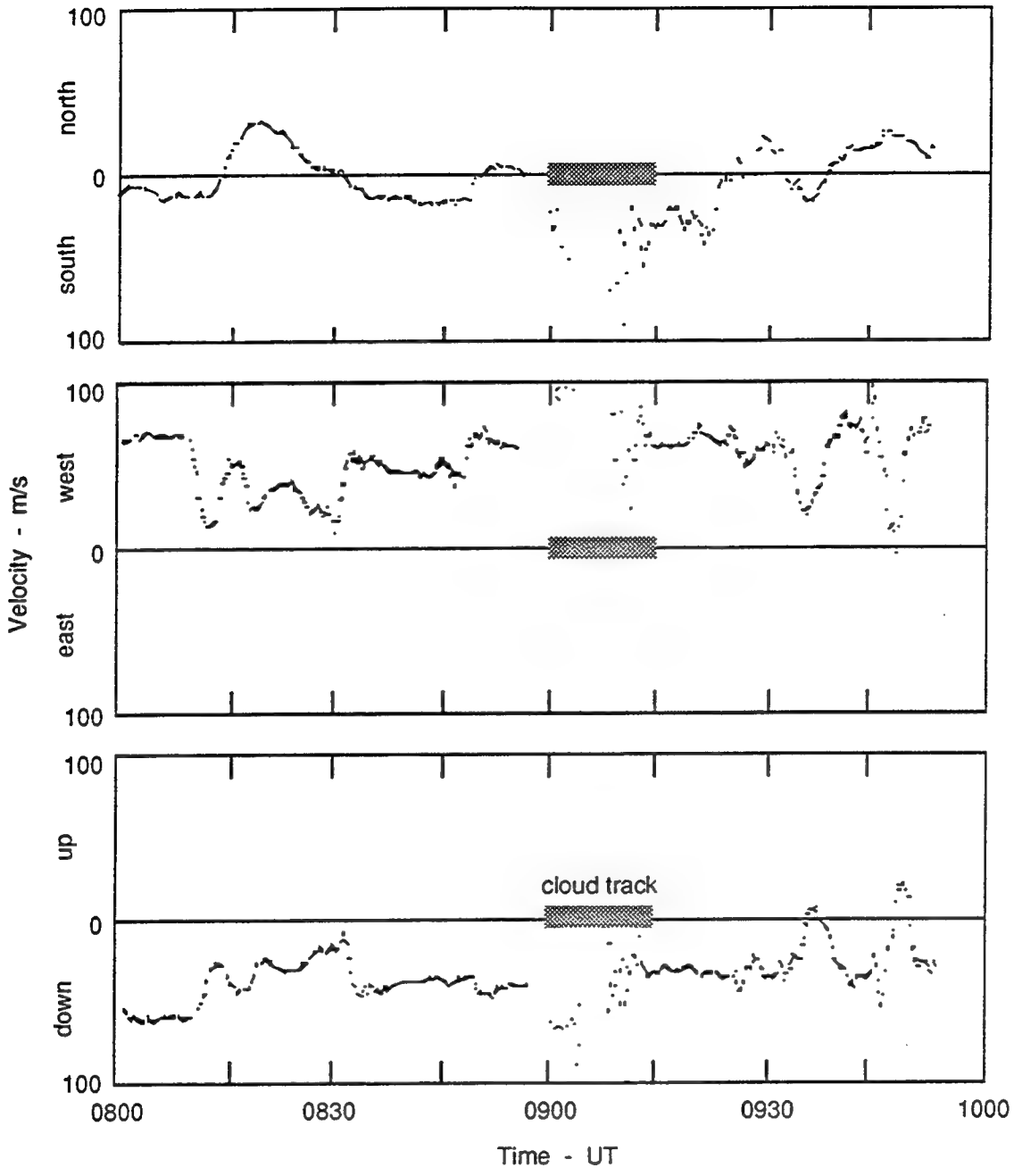

Figure 1 RESOLVED PLASMA DRIFT IN MAGNETIC COORDINATES MEASURED BY THE ARECIBO RADAR, JULY 2, 1992

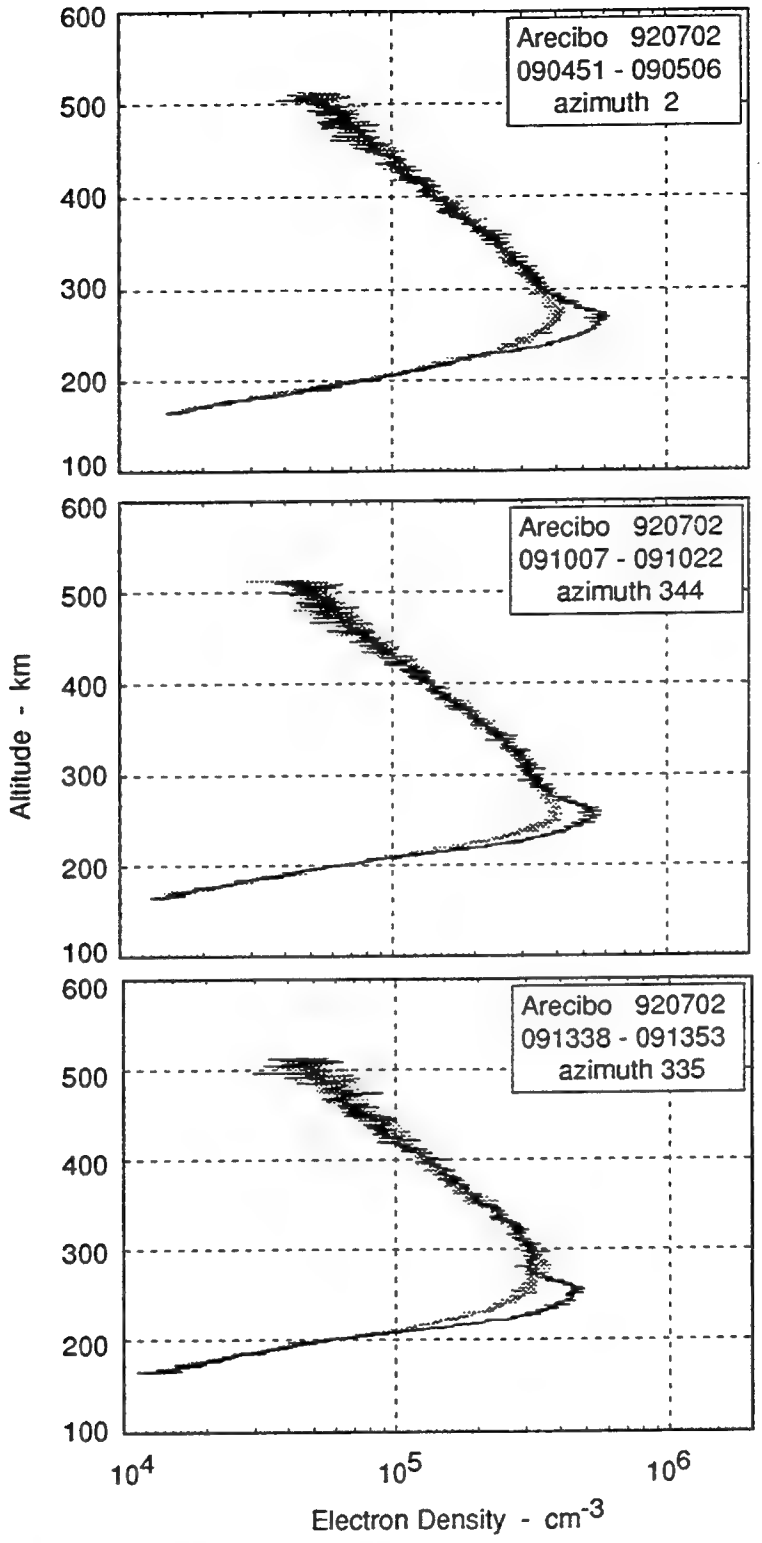

Figure 2 ELECTRON DENSITY PROFILES MEASURED BY THE ARECIBO RADAR AFTER CRRES RELEASE AA-1, JULY 2, 1992

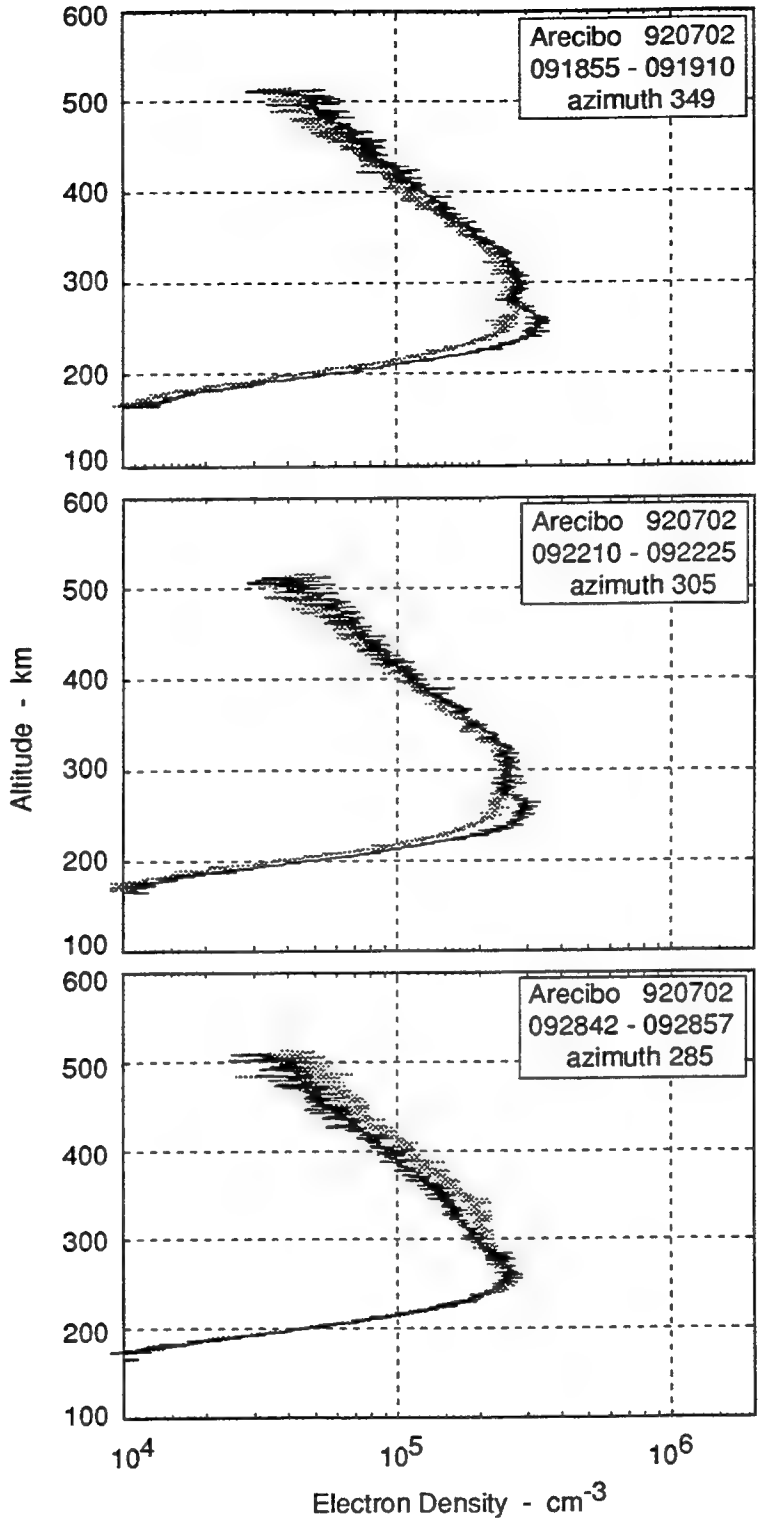

Figure 2 ELECTRON DENSITY PROFILES MEASURED BY THE ARECIBO RADAR AFTER CRRES RELEASE AA-1, JULY 2, 1992 (concluded)

2.2 JULY 4 RELEASE

The second PL rocket (AA-7) payload was released at 254 km on July 4, 1992, at 0858 UT. The background F layer was slightly higher in altitude and in peak density than it was on July 2. Although the overall drift of the cloud was to the west/southwest, the measured F region plasma drifts were much more variable than they were on July 2. Launch was preceded by almost an hour of low, but structured background flows. Such short-term variations in electrodynamic forces may be the reason that the plasma cloud is less clearly defined in the sequence of electron density profiles shown in Figure 3. For each scan, the cloud is discernable from the change in shape of the background profile that it creates, rather than a distinct enhancement in electron density. In fact, in the three scans after 0910 UT, the cloud perturbation appears as an apparent depletion of electron density relative to the background profile measured a short distance away to the east or west.

2.3 BARIUM CLOUD DYNAMICS

The small-scale dynamics within or around a barium cloud release have not been studied, although it has been predicted (Drake *et al.*, 1989) that a cloud released at these altitudes will rotate. This rotation is in response to a combination of factors involving the height-integrated conductivity and background plasma drift. The CRRES releases, tracked by the Arecibo radar, provided a unique opportunity to study the early time cloud dynamics and to test the rotation prediction.

Figure 4 shows the line of sight velocity patterns observed during three azimuth scans through the cloud between releases at 0903 UT and 0921 UT. The traditional incoherent scatter convention is used here so that a positive velocity is away from the radar. The velocity is derived from ACFs that have been integrated 15 seconds in time; because the antenna is constantly moving, each velocity point corresponds to several degrees in antenna azimuth. The ACFs are also integrated in range, providing an effective gate width of 16 km centered at an altitude of 251 km. The cloud was dropping slightly in altitude during this time, but this range remains well within the cloud. For all three scans the electron density in the same range gate is plotted to illustrate that the spatial resolution of the velocity measurements is good relative to the overall dimensions of the barium cloud.

There is significant variation in the observed line of sight velocities that is, in part, due to the relatively low electron density of the early morning ionosphere. Furthermore, the velocity shown here was derived from phase rate estimates determined from the first few legs of the measured ACFs. These may be noisier than those obtained from a more complete fit analysis of the ACFs. The fit approach is also preferable in that it provides statistical confidence intervals to the velocity estimates.

The transmitter at Arecibo imparts a slight Doppler shift to the signal that needs to be removed to obtain true line of sight velocity estimates. The chirp has been removed from the line of sight velocities that were resolved into vectors for Figure 1, but not from the data shown in Figure 4. The background ionospheric drift creates the azimuth-dependent component in the figure, which is indicated by the smooth line. This was derived from range-integrated ACFs in the vicinity of the cloud and remains nearly constant throughout the three scans shown here.

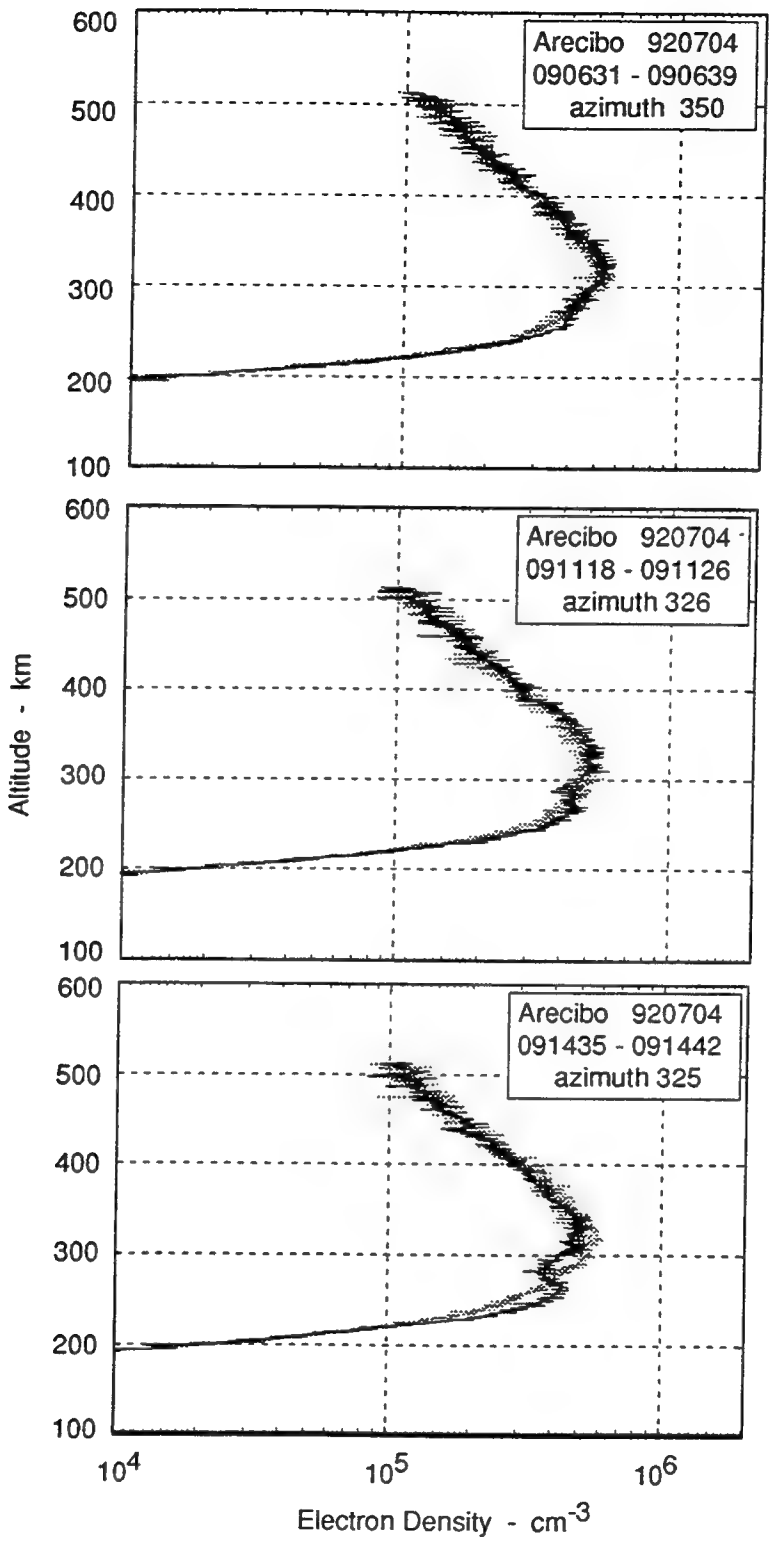

Figure 3 ELECTRON DENSITY PROFILES MEASURED BY THE ARECIBO RADAR AFTER CRRES RELEASE AA-7, JULY 4, 1992

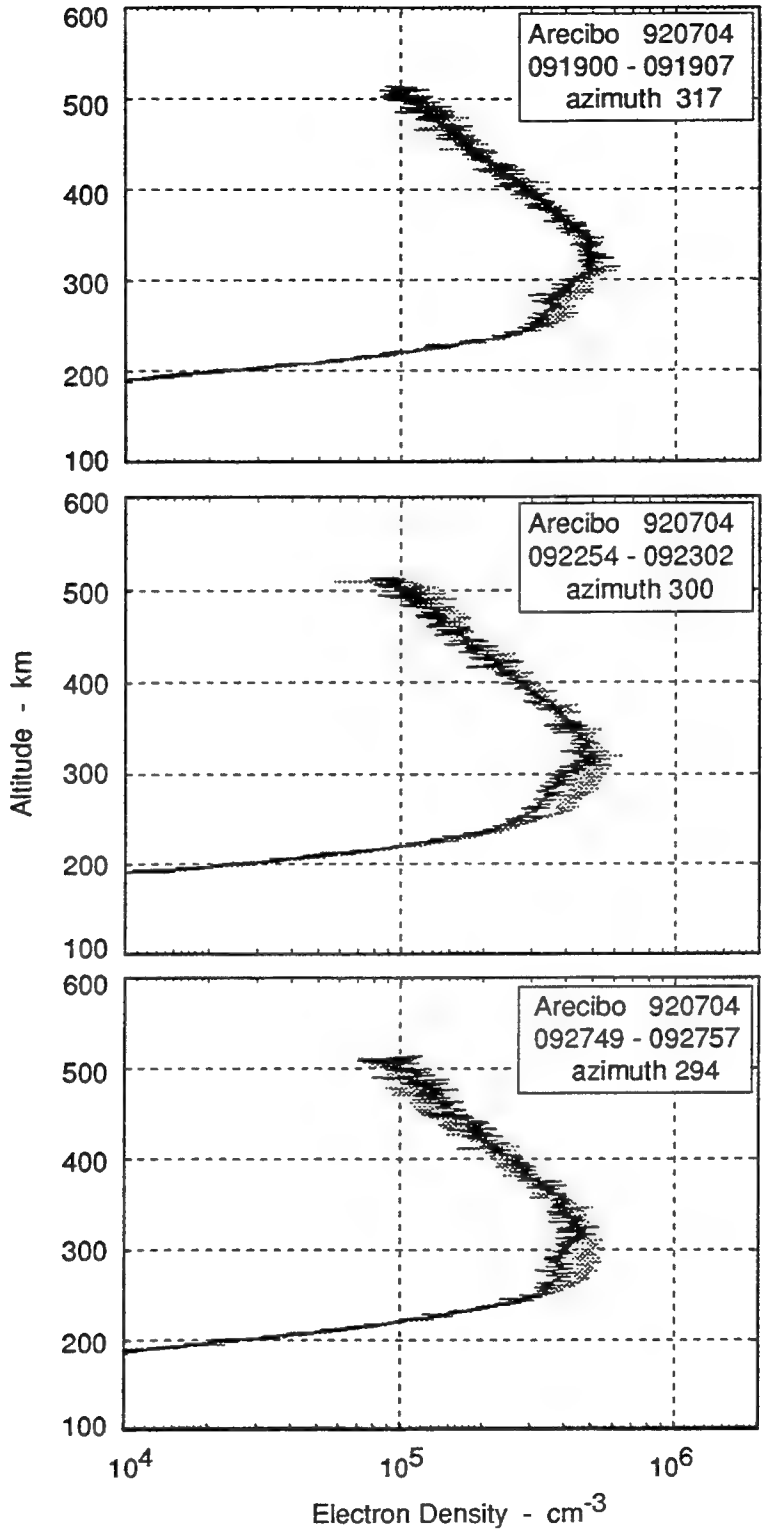

Figure 3 ELECTRON DENSITY PROFILES MEASURED BY THE ARECIBO RADAR AFTER CRRES RELEASE AA-7, JULY 4, 1992 (concluded)

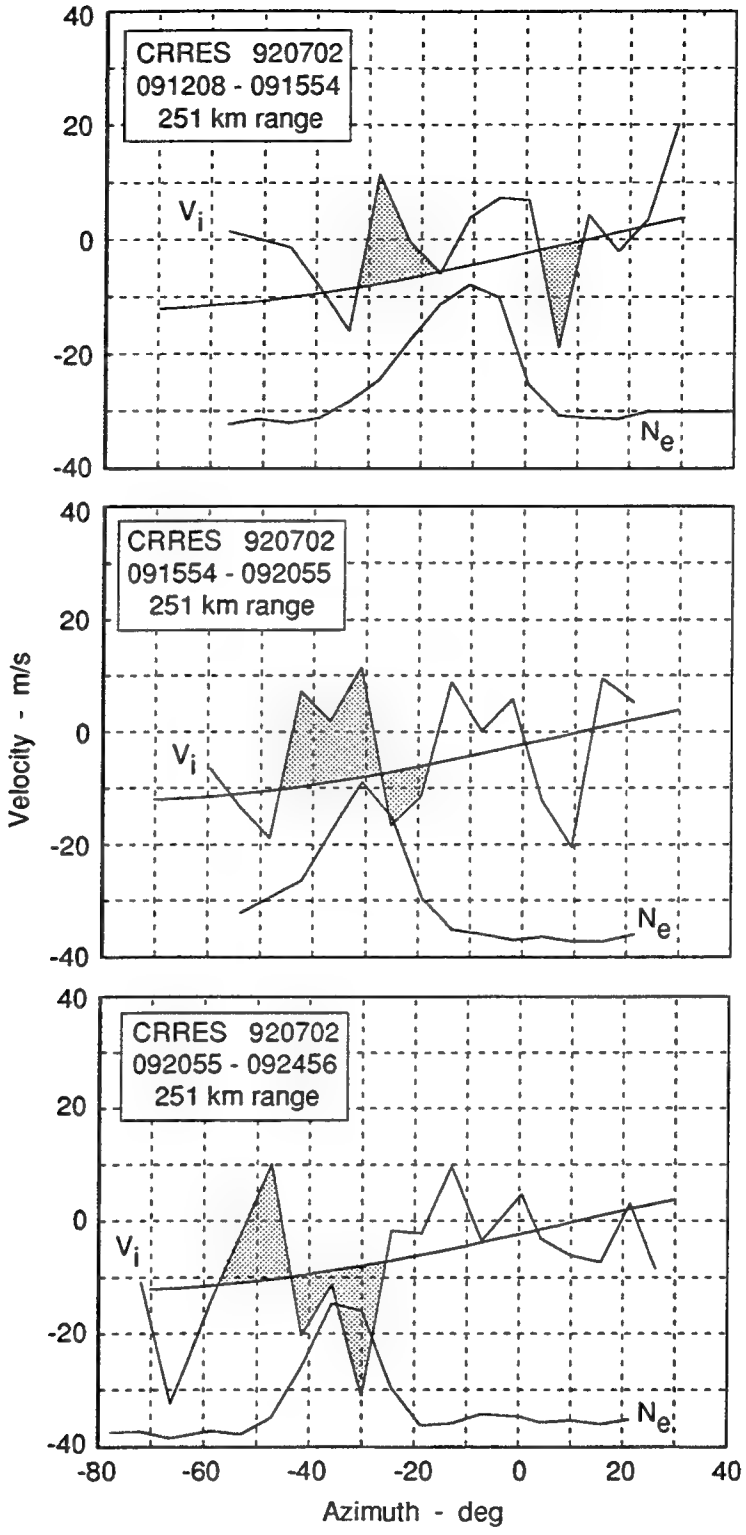

Figure 4 LINE OF SIGHT VELOCITY AND ELECTRON DENSITY MEASURED BY THE ARECIBO RADAR DURING SCANS THROUGH THE AA-1 BARIUM CLOUD, JULY 2, 1992

There is some suggestion in the data from the 0912 to 0915 UT scan that the outside edges of the cloud are rotating. The westward and eastward edges are moving away from and toward the radar, respectively, at an apparent velocity of about 20 m/s relative to the background. The regions of the peak velocity are well separated from the high density portions of the cloud, which is in good agreement with the Drake *et al.* (1992) model. It is difficult to accurately estimate the dimensions of this rotating "shell" because the cloud is both drifting and expanding during the radar scan, but its extent in azimuth suggests a radius of at least 50 km. At even a very slow cloud rotation rate the angular velocity of the plasma in so large a shell is likely to be large. However, the radar sees only the component of the rotation perpendicular to its line of sight. Furthermore, the temporal and spatial smearing inherent in the azimuth scan might well produce a collective Doppler estimate that is much smaller than the peak drift in a narrow shell region. Whether the observations, with these factors considered, are consistent with the Drake *et al.* (1992) prediction has not been addressed.

The same simple rotational characteristic is not seen in the two subsequent scans through the cloud. There are regions of negative velocity, but they appear to fall within the cloud rather than on its eastward edge. However, there is a consistent region of significant positive velocity that is associated with the westward edge of the barium cloud for all three scans. There is no obvious explanation for the evolution from a simple rotating cloud to a configuration that would produce the velocity pattern seen in the figure. There is evidence from other instruments that the downwind edge of the cloud had steepened in response to neutral wind-driven polarization fields, and this may play a role in altering the cloud rotation process. Steepening can also lead to bifurcation of the cloud into two lobes, as was observed during the SECEDE II experiments. Detailed analysis of these data need to be completed to determine the cloud configuration. The radar data from the July 4 and July 12 releases also require further review to determine similar evidence of cloud rotation or one-sided shear regions.

2.4 BARIUM CLOUD COMPOSITION

In addition to being used to derive electron density, N_e, and the velocity of the plasma ions, V_i, the ACF of an incoherent scatter radar return contains information about its plasma composition and the electron and ion temperatures, T_e and T_i. The CRRES releases within view of the powerful Arecibo Observatory provided a unique opportunity to study, in some detail, the composition of the barium releases as they evolved in time. The signal returns from the cloud have a relatively high signal to noise ratio (SNR) because of the large antenna at Arecibo, which is of significant benefit to the analysis. The detailed analysis to obtain plasma composition is still difficult, however, and involves fitting, in a non-linear least-squares sense, the measured ACF to a theoretical function of electron density, electron and ion temperatures, collisions, and ionic composition (Zambre, 1993). At the altitude of the CRRES releases, ion-neutral collisions are not of concern, but there are functional ambiguities between temperature and composition mixes, both of which affect the shape of the ACF.

Initial attempts at fitting the Arecibo ACFs was done without constraints or assumptions, other than specifying a mix of O^+ and Ba^+ ions, and assuming that the ion and electron velocities were equal. Despite the high percentage of barium known to be in the cloud, the unconstrained fitting process converged on an excellent solution for O^+ only, but at unrealistic values of T_e and T_i. Clearly, some constraints had to be placed on the fitting process if any information about the

mix of O^+ and Ba^+ was to be obtained. The first assumption made was that the electron temperature, T_e, in the cloud was the same as that derived from the background ionosphere in the vicinity of the cloud. This is likely to be the case, particularly during the first tens of minutes after release at an altitude of 250 km. The second assumption was that the ion temperature, T_i, was the same as that of the electrons. The results suggest that this is probably not a particularly good assumption, but it is a necessary one in order to obtain initial estimates of composition. With these constraints, the fitting was reapplied to the data, solving for N_e, $T_i = T_e$, $V_e = V_i$, and composition. The results from the fit to the July 2 (AA-1) release for the three early scans through the cloud between release and 0914 UT are shown in Figure 5.

Three of the contours in Figure 5 are of the derived percentage Ba^+ ions in the cloud as a function of the antenna azimuth. The patterns show a reasonable spatial pattern for the cloud as it drifts westward in time. In each, the peak percentage of Ba^+ is as indicated, and occurs consistently in the center portion of the cloud that was scanned. This rises with time, as would be expected, as the molecular barium is ionized by solar EUV radiation. Although a formal confidence analysis has not been made, these percentages are likely to be somewhat high and need to be considered in light of the assumptions made in the fitting process. One check on the consistency of the fits to Ba^+ is to derive the background O^+ number density within the cloud volume; this is shown in the bottom right panel of the figure. This would not have changed in response to the barium release if the assumptions were correct that T_e and T_i were equivalent and unchanging. Unfortunately, the pattern of O^+ number density clearly shows the image of the cloud, with a significant drop in the regions of significant Ba^+.

This preliminary analysis is incomplete, but shows the potential of using the radar to diagnose the ionization process within the cloud. Analysis of these data and of those from the other two releases could be refined by using estimates of ionospheric parameters from other techniques and instruments. The electron density within the cloud is very precisely measured by simultaneous plasma line observations (Djuth *et al.*, 1993), which reduces one degree of freedom in the fitting process. Furthermore, the comparison of that density to the raw ion line density can be used to obtain the ratio T_e/T_i. A less important component of the fit is the ion velocity, which has been discussed in the previous paragraphs and can be confirmed using the optical images of the barium cloud obtained during the first minutes after release. With the fitting process thus better constrained, a comparative study of Ba^+ evolution in two non-heated releases and the heated AA-2 release, would be particularly interesting.

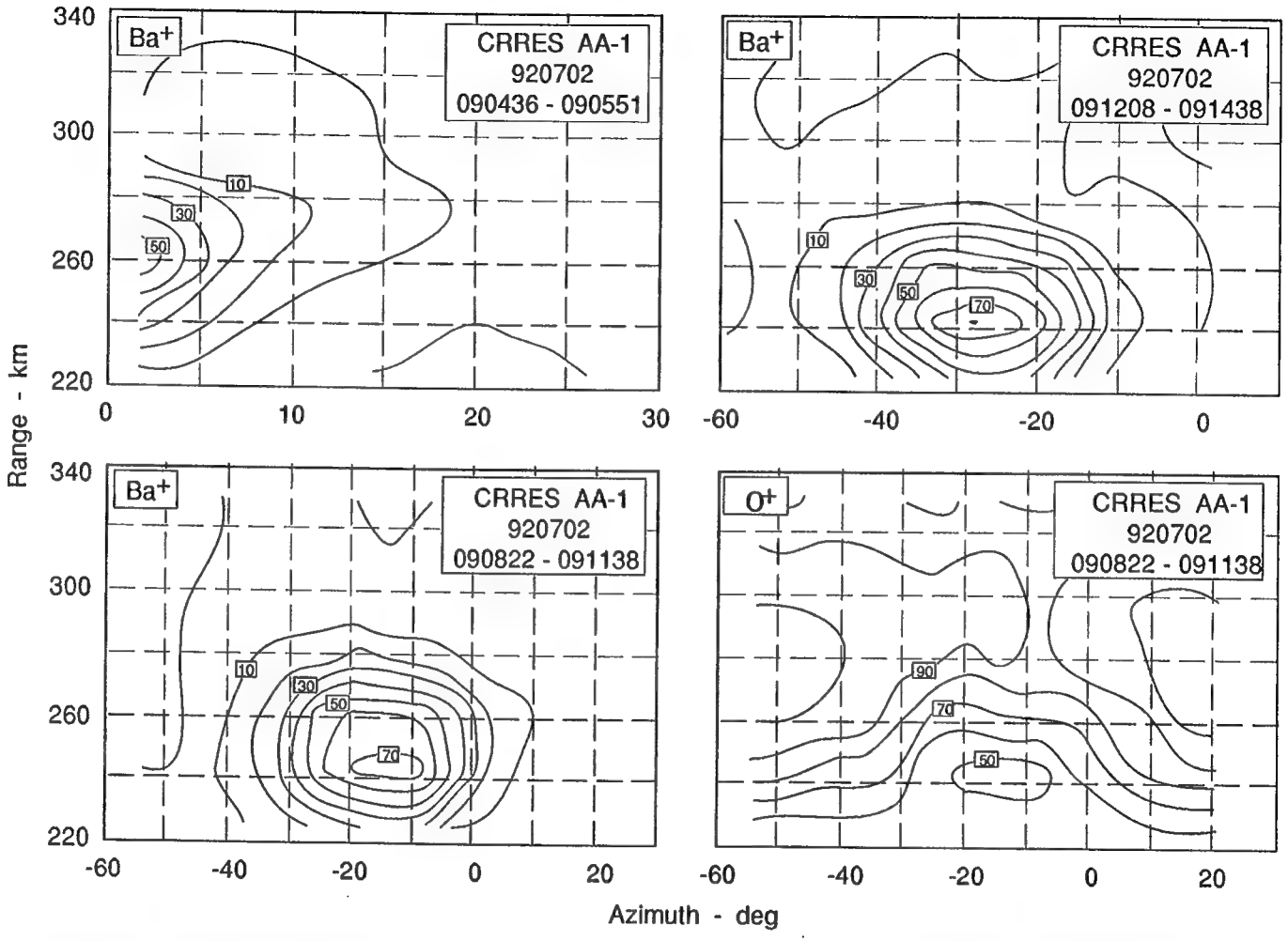

Figure 5 CONTOURS OF BA^+ and O^+ COMPOSITION DERIVED FROM ARECIBO RADAR DATA, RELEASE AA-1, JULY 2, 1992

3 HIGH FREQUENCY RADAR MEASUREMENTS

The SRI FAR is a portable system that operates between 2 and 50 MHz and is readily adapted for multiple uses (Tsunoda *et al.*, 1993). Its application for CRRES was to characterize the image structure in the lower ionosphere below the cloud, and to generally diagnose the barium cloud and its dynamics.

Images are formed by the non-uniform polarization electric fields that surround striations within the barium cloud; these effectively map down to the lower ionosphere and form a region of mirrored structure. The mapping is efficient only at spatial scales larger than a few hundred meters, which makes direct measurement of images using HF radar difficult, since the lowest practical operating frequency (in terms of antennas) is about 2 MHz. At this frequency, field-perpendicular backscatter would arise from relatively small irregularities, those with a 75-m cross-field spatial scale. It was anticipated, however, that the much larger image irregularities might structure from secondary instabilities, such as the gradient-drift process that creates mid-latitude sporadic E. Accordingly, the FAR was operated from the Los Canos site, not far from the Arecibo Observatory. Magnetic field-line tracing from the nominal cloud release location showed that direct magnetic perpendicularity from Los Canos occurred at an altitude of 130 km, the near-optimum altitude for image formation. If the images were to form and secondarily to structure, the FAR would observe them a few minutes after release.

The FAR was also tasked to generally characterize the barium cloud and its motion. Very high peak plasma densities were expected to occur in the barium ion cloud, so overdense reflections from the cloud at relatively high frequencies (up to 30 MHz) were anticipated. Using the frequency agility of the FAR, a collection of frequency control files was prepared that would lower the radar frequency as the ion cloud diffused. This would provide a time history of the maximum plasma density of the ion cloud until it reached a plasma density of about 1×10^5 el/m^3.

It was also expected that coherent backscatter from irregularities within the cloud could be observed starting some tens of minutes after release. At the nominal time of release, the ionospheric electron density at Arecibo is typically quite low (Shen *et al.*, 1976). However, the background density rises quickly after sunrise, and ray-tracing analysis showed that within about 30 minutes there is sufficient ionospheric refraction to obtain magnetic orthogonality at the cloud. It was planned to compare these backscatter measurements with those obtained by CUPRI at 50 MHz from St. Croix, since there exists virtually no data on the frequency dependence of field-perpendicular backscatter at meter- to decameter-scale sizes.

For CRRES, the FAR was configured to operate at 16 kW peak power, using a 7-baud Barker-coded waveform with a 20 μs (3 km range resolution) sub-pulse. Crossed delta antennas were utilized so that the FAR could operate over the wide frequency range anticipated for over-dense returns from the barium cloud. There were two operational modes that were exercised: an ionosonde mode and a fixed-frequency Doppler mapping configuration. Each morning of the campaign, prior to the opening of the rocket launch window, the FAR operated in an ionosonde mode to search for quiet frequencies within the HF band. Because of the high peak densities

expected for the large volume releases, 19 standard operating frequencies between 2.24 MHz and 28.94 MHz were chosen. This range was reduced to a maximum frequency of 12.94 MHz after observation of the low peak density yield of the July 2 release.

When operated in an ionosonde mode, the FAR data can be used to estimate the peak ion density associated with the cloud. An ionogram from the July 4 launch, some 15 minutes after cloud release, is shown in Figure 6. There is a weak sporadic-E layer at about 100 km altitude, and the O- and X-mode traces of signals reflected from the background F layer. In between are the overdense echoes from the barium cloud seen at a virtual height of about 230 km. These extend out, unambiguously, to a frequency of about 5.5 MHz, with some suggestion of the return out to about 5.7 MHz. This highest frequency corresponds to the smallest cross section measurable by the FAR, and is the size of the isodensity surface in the cloud associated with that plasma frequency. This corresponds to a peak ion density of 3.9×10^5 el/m^3, which compares reasonably well with the value obtained by the ISR.

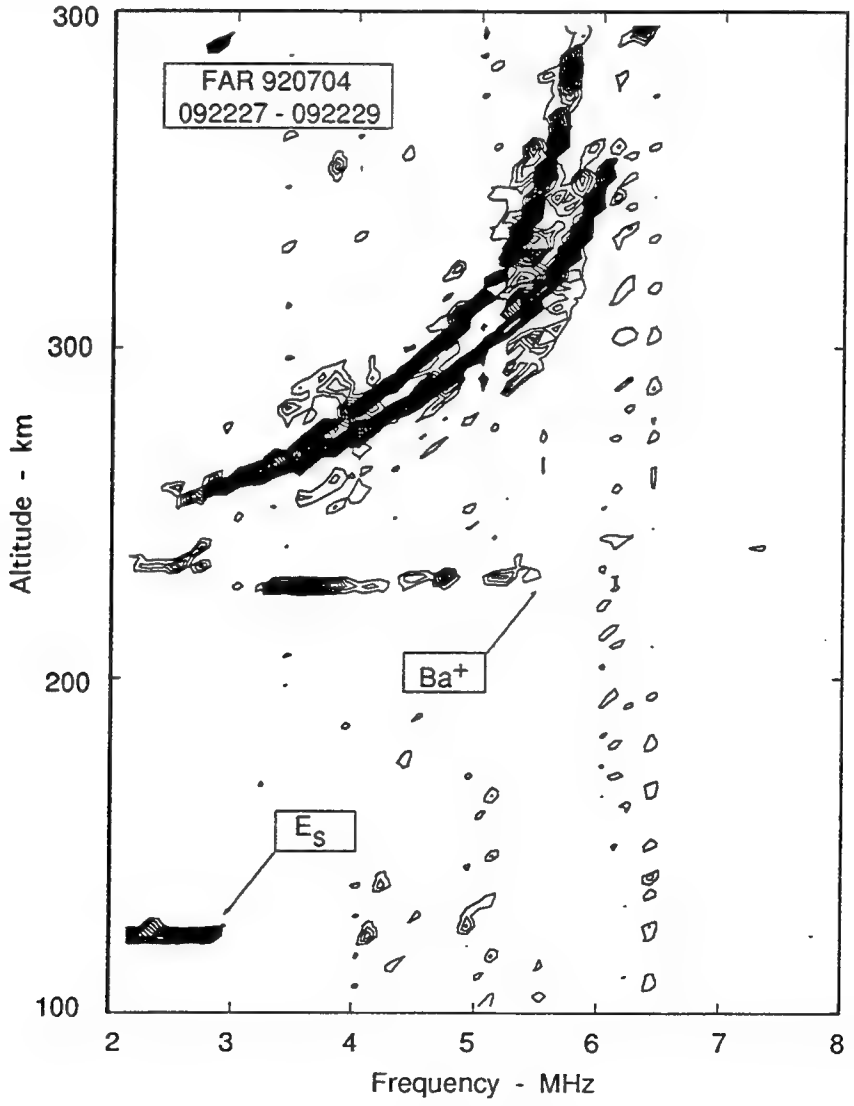

Figure 6 IONOGRAM MEASURED BY THE FAR AFTER CRRES RELEASE AA-7, JULY 4, 1992

Normally the FAR was operated in a Doppler dwell mode, producing range-Doppler maps at a number of operating frequencies. The maps are derived from pulse-to-pulse processing, using a pulse repetition frequency (PRF) of 100 Hz. This rate is adequate to resolve cloud motion exceeding about 200 m/s at an operating frequency of 5 MHz. On July 2, the initial cycle of 19 frequencies showed no evidence of image formation, although direct overdense returns from the ion cloud were seen up to a frequency of 7.14 MHz. The range-Doppler map taken at 8.84 MHz shortly after release showed no return, implying a peak ion density with a plasma frequency between 7.14 MHz and 8.84 MHz, i.e., a maximum ion density less than about 1×10^6. The coincident incoherent scatter observations reviewed in Section 2 are consistent with this observation, indicating a peak electron density at 0910 UT of 6×10^6 el/m^3, or a plasma frequency of about 7.5 MHz.

Examples of the range-Doppler maps for the July 2 release are shown in Figure 7. Returns are shown from three different frequencies (5.64, 6.64, and 7.14 MHz) just after release, and at the same frequencies some 40 minutes later. The convention for velocity sense is opposite that for the ISR radar, that is, negative Doppler velocity is away from the FAR. Some information about the cloud characteristics can be gleaned from the echo patterns in the range-Doppler maps of Figure 7. Those at 6.64 MHz and 7.74 MHz at the earlier time are good examples of reflections from a relatively smooth cloud. The three weaker discrete echoes that appear on either side of the maximum return are range sidelobes produced by the phase coding of the transmit pulse. Their appearance in the returns suggests that the cloud remains a single and constant specular reflector throughout the mapping period. There is some Doppler spreading in the main echo at 6.64 MHz and 7.14 MHz; this is likely sidelobe energy caused by a slow change in echo power over the measurement interval, but could suggest some minimal structuring within the cloud. The Doppler maps at 0945 UT are near-duplicates of the earlier returns, and illustrate that even slow structuring processes in the cloud were suppressed.

The early-time range-Doppler map at 5.64 MHz is noticeably more distorted and spread than those at the two higher frequencies. The spreading is likely a result of the rapid time evolution of the plasma cloud during its formation phase before diffusive equilibrium is reached. During this phase, the barium expands along the magnetic field at a rate comparable to the pulse-to-pulse observation interval. The expansion velocity, rather than the presence of structure, could readily explain the Doppler spreading of the return.

The primary returns in the range-Doppler maps provide an accurate measure of the range and drift of the cloud, and thus provide an opportunity to track its motion for an extended period. This was useful for CRRES because it includes times after dawn when optical sensors are no longer useful, and times when the cloud was below the minimum elevation of the Arecibo radar.

Figure 8 shows a track of the July 2 release in terms of Doppler shift and group path range, scaled from the sequence of 5.64 MHz range-Doppler maps. A consistent correspondence is seen between the cloud motion and its range. The range minimizes at about 0924 UT, indicating that the ion cloud was at closest approach to the FAR, and at this same time, the Doppler shift crosses from positive to negative. Positioning information of this type is useful in conjunction with other non-collocated instruments, such as the Ramey Digisonde. If spaced-antenna measurements had been available, actual angle of arrival versus time could have been made, allowing single-station three-dimensional tracking.

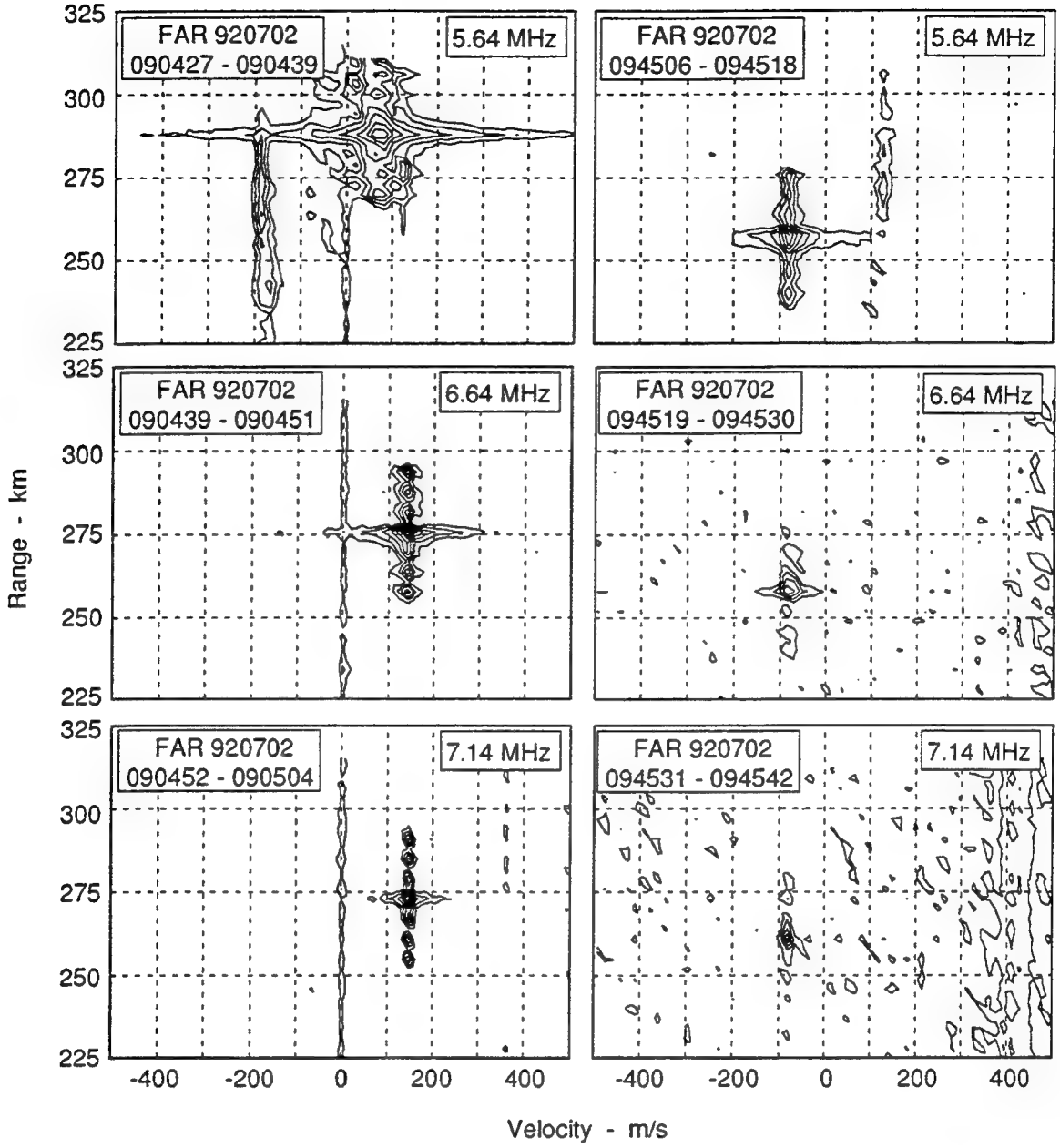

Figure 7 DOPPLER MAPS OF THE AA-1 BARIUM CLOUD MEASURED BY THE FAR, JULY 2, 1992

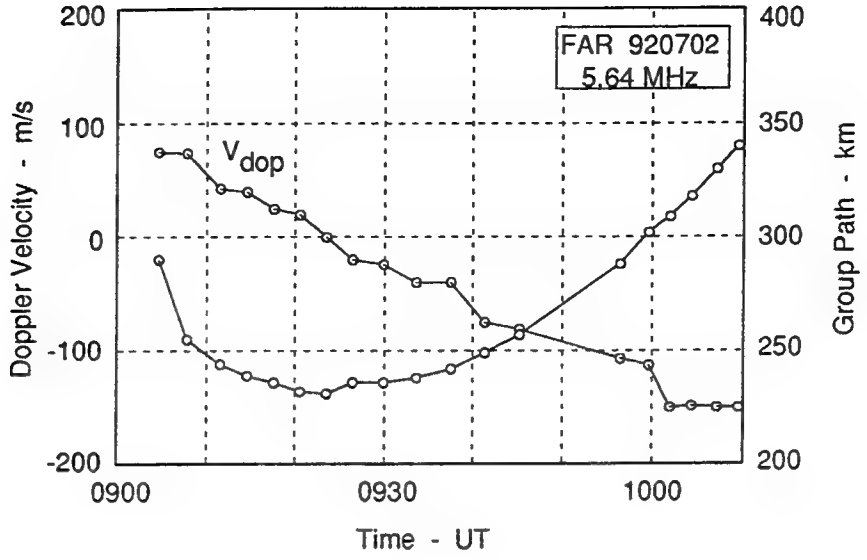

Figure 8 RANGE AND DOPPLER MEASUREMENTS OF THE AA-1 BARIUM CLOUD MADE BY THE FAR, JULY 2, 1992

The Doppler maps collected by the FAR during early development of the cloud are of interest, particularly in light of the velocity structure seen by the incoherent scatter radar. Figure 9 is a sequence of three maps collected at 6.64 MHz between 0907 and 0918 UT for the July 2 launch. All show the compact return signature of the barium cloud drifting with a positive Doppler, toward the FAR. Additionally, at the same range as the cloud, a compact second return appears with a high Doppler shift. The velocity is initially very high, nearly 300 m/s at 0907 UT and is seen at both positive and negative frequencies, much as if the cloud were rotating. In subsequent frames, only negative offset returns are observed, and these systematically decrease to less than 100 m/s by 0918 UT. Similar, but much weaker returns are seen in the Doppler maps at 5.44 and 7.44 MHz.

The large magnitude of the Doppler shifts could be from structure within the cloud, or it might be a product of an HF propagation process that enhances the Doppler shift. For example, chordal modes of propagation along fingers of ionization have been identified as possible explanations for anomalously high Doppler shifts during other HF radar studies of barium clouds (Waterman *et al.*, 1972). Alternatively, the high offset Doppler might be from the shear "shell" suggested to explain the consistent high-velocity region on the westward edge of the July 2 barium cloud. As has been noted, even at slow rotation rates, the large radius of the cloud would produce high Doppler shifts for returns from its edge. Also, it is probable that the rotation rate will slow as the barium diffuses and/or as the lower ionosphere becomes sunlit, much as the data in Figure 9 indicate. In either case, it is likely that the large negative Doppler shifts seen by the FAR are associated with the velocity patterns seen by the ISR, and shown in Figure 4. Analysis of the July 4 release data needs to be completed to see if similar offset returns are seen by the FAR.

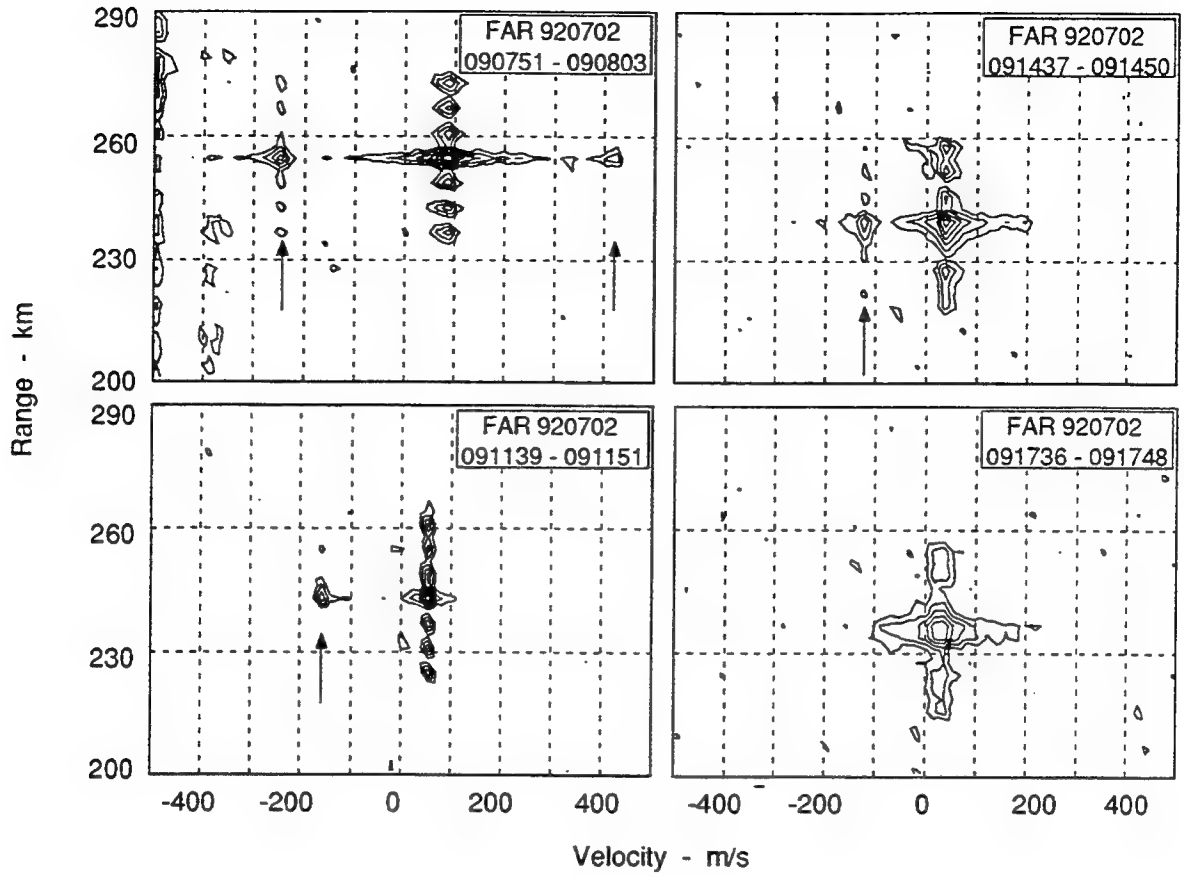

Figure 9 **DOPPLER MAPS OF THE AA-1 BARIUM CLOUD MADE BY THE FAR SHOWING HIGH VELOCITY OFFSET RETURNS, JULY 2, 1992**

4 TRANSIONOSPHERIC SCINTILLATION MEASUREMENTS

The phase of a UHF satellite signal passing through the ionosphere is altered by the refractive index of the dispersive plasma, with the amount of phase path change proportional to the integrated electron density (TEC) along the propagation path. Processes such as heating or chemical releases alter the TEC and therefore can be diagnosed using satellite signal paths to ground-based receivers. If the modification processes directly or secondarily create electron density irregularities, information about the irregularities can be derived from the scintillation data.

In actuality, the ionosphere is not uniform in electron density, but is constantly altered by a variety of processes. At the slowest time scales, large-scale tidal and wave fluctuations alter the TEC, electrodynamic processes alter the density distribution at tens of kilometers scales, and convective instabilities can act to produce meter-scale irregularities. The result is an *in-situ* spectrum of electron density that extends from hundreds of kilometers through meter spatial scales, with an approximate power-law form. The largest electron density irregularities affect just the phase of a propagating signal, but those smaller than a Fresnel scale (a few hundred meters at UHF) diffraction can also alter the signal amplitude. For the weak irregularity strength conditions of interest here, there are no diffractive effects in either amplitude or phase. Phase screen theory (e.g., Rino, 1979) shows that under such conditions the phase spectrum received at a ground receiver can be directly related to the spectrum of the *in situ* irregularities.

Interpretation of phase scintillation data is complicated because it is a result of the integrated effects of electron density structure along the entire signal path, and includes contributions from different altitudes. Furthermore, the phase deviations are proportional to ΔN^2, so that the phase spectrum typically reflects structure at the peak of the ionospheric F layer. For a signal path through the chemical release cloud, the phase data provide a direct diagnostic of the structure within the cloud, because the electron density is higher than that of the background ionosphere. However, the phase scintillation during heating is less simple to analyze: a signal path directly through the heated volume might show less scintillation then does one that penetrates altitudes where the perturbation percentage is smaller, but the background density is higher.

For CRRES, measurement of propagation effects produced by the barium cloud required mobility of the UHF receiver, so the scintillation receiving system installed on the Phillips AIO aircraft was utilized. The collection of complex signal scintillation from aboard an aircraft is complicated by the motion of the vehicle. For the equipment on the AIO, the phase of the signal is derived by very precise tuning of the receiver to the stable satellite signal source. The Doppler shift due to overall aircraft motion is constant and is of no consequence, but any random deviation of the aircraft from straight-and-level flight will induce a geometrical Doppler that cannot be distinguished from ionospheric dispersive phase. During turbulence, for example, a weak-scatter phase spectrum can become masked by energy from the rapid movement of the aircraft. Fortunately, the CRRES flights (with minor exceptions) were all made under very smooth flight conditions.

The flight path of the AIO on each evening was planned to maintain a "racetrack pattern" for some period prior to rocket release, and then, directed by ground sensors, to track and make multiple scintillation passes through the cloud. The racetrack was laid out to place the scintillation path within the volume heated by the Islote Heater, in order to make measurements of heater-produced thermal self-focusing irregularities, independent of the barium cloud observations.

4.1 CLOUD MEASUREMENTS

During the planning of the CRRES rocket releases, it was anticipated that the high-volume barium ion cloud would rapidly expand and striate. If this were the case, stria with cross-field dimensions on the order of a few hundred meters would form; these are known to produce strong scintillation at UHF frequencies (Burns and Livingston, 1972). Multiple scans through the cloud would characterize the growth and decay of the irregularity spectrum, which are important aspects of the plasma structuring process. The AIO experiments were designed to take advantage of the mobility of the aircraft to make as many scans as possible through the structured cloud as it developed, drifted, and decayed.

As noted above, none of the three CRRES barium releases structured at intermediate scales (or even at smaller scale sizes). This made the task of using the airborne scintillation data to detect the ion cloud in real time much more difficult. In the absence of scintillation-producing structure, the signature of the barium ion cloud is limited to that produced by the change in TEC along the raypath as the cloud is traversed. The peak electron density in the clouds was also only slightly larger than that of the background ionosphere, making it difficult to separate background large-scale dispersive changes from those produced by the release, per se.

Figure 10 is one example of the propagation effects created by intersection with the cloud. It shows the amplitude and phase of the satellite signal during the initial intersection with the July 12 barium cloud. The raypath entered the southwestward edge of the cloud at about 0908 UT, approximately 5 minutes after barium release. The perturbation in signal amplitude that is seen is typical of the diffraction signatures produced by a sharp gradient in TEC. In principle, the TEC gradient can be derived from this pattern of the complex signal (Gagnon, 1964). The cloud was drifting primarily westward at this time, and the intercepted edge of the cloud was likely to be steepening as it drifted westward in the presence of a south-westward neutral wind.

The phase pattern in Figure 10 also shows the change of TEC that is attributable to the cloud, if some assumptions are met. The background ionospheric TEC is assumed to be constant over the duration of the scan, which is likely to be the case. However, the scan in the figure is not a snapshot of the cloud, but takes about three minutes to complete. If the cloud was not rapidly evolving, the TEC pattern suggests that it was not spherical, but instead consisted of two lobes. There was similar large-scale bifurcation at early times of some clouds in the SECEDE series of barium releases (Linson, 1972). It could also be argued that the observed TEC signature is of the cloud distorted by time, i.e., the raypath first passes through the center of the cloud, which then drops in altitude, but subsequently expands into the raypath again.

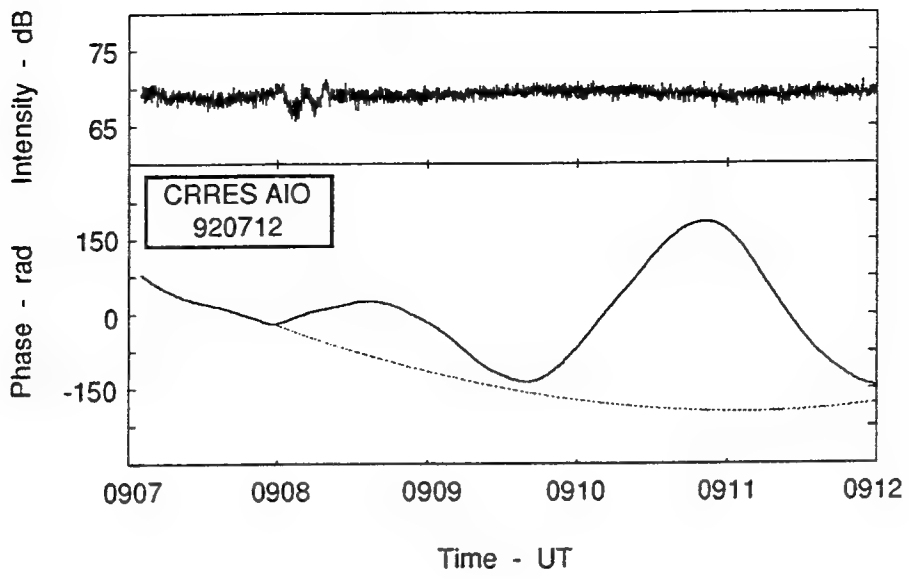

Figure 10 UHF TRANSIONOSPHERIC SIGNAL INTENSITY AND PHASE MEASURED AT THE AIO DURING THE INITIAL INTERSECTION WITH THE AA-2 RELEASE, JULY 12, 1992

The dispersive phase change in Figure 10 is directly proportional to the change in TEC encountered along the raypath. The 300 radian offset at the higher peak corresponds to a change in TEC of approximately 1×10^{17} el/m^2. If it is assumed that the barium cloud is Gaussian in shape and approximately 50 km in diameter at this time, this added TEC corresponds to a peak density of about 7×10^5 el/cm^3 at the center of the cloud. For the portions of the July 2 and July 4 clouds that were measured by ISR, the peak densities (without temperature or composition correction) were close to 2.5×10^6 el/cm^3 so this value is within reason.

The top panel in Figure 11 shows the signal response to the intersection with the July 2 cloud. The diffraction signature in amplitude is significantly weaker than on July 12, perhaps because the cloud was intersected about 20 seconds after release and had not yet begun to steepen. The phase signature in this case is more difficult to interpret because the aircraft began a turn at 0906 UT. At this very early time, the cloud was still extremely compact (approximately 25 km wide), producing a change in TEC of 7×10^{16} el/m^2.

Signal path intersection with the AA-7 release cloud also occurred very soon after release, and the aircraft data show a similar signature of the cloud. The one difference is that the amplitude focus occurs on the northeast edge of the cloud. This is likely attributable to a difference in the direction of neutral wind, which acts to build polarization fields and steepen the edges of the cloud. The change in TEC along the propagation path during passage through the cloud is remarkably similar between the two days. To illustrate the similarity of the amplitude and dispersive phase, the July 4 data are reversed in time in the bottom panels of Figure 11. Alignment of the cloud edges in phase also aligns the amplitude structure.

There are several other examples of phase structure in later flight legs on July 2, 4, and 12 that are presumably intersections with the cloud. The propagation geometry and cloud position are known accurately enough so that these data could be usefully analyzed (for example, to estimate the barium cloud density gradient as a function of time).

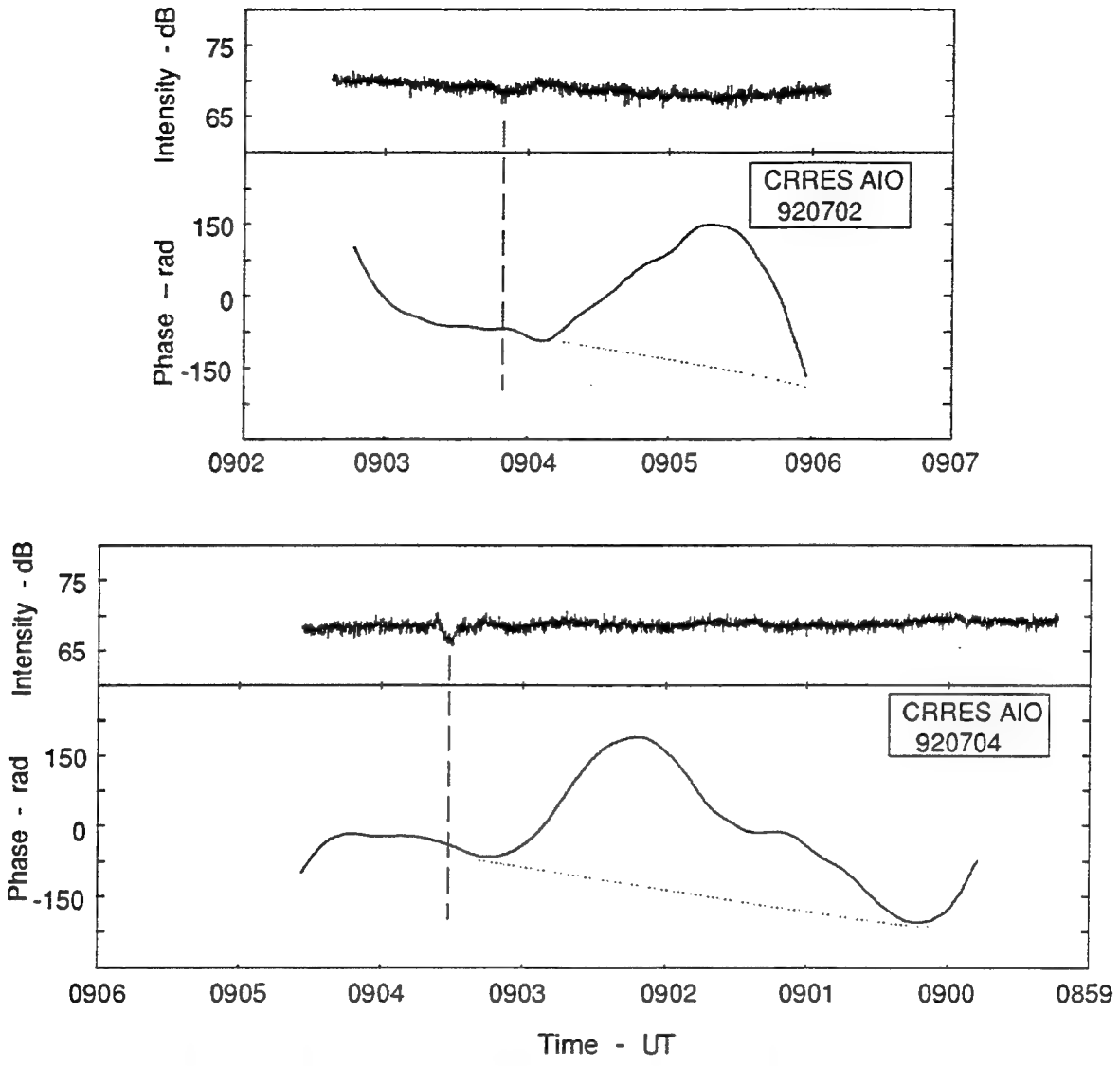

Figure 11 UHF TRANSIONOSPHERIC SIGNAL INTENSITY AND PHASE MEASURED AT THE AIO DURING THE INITIAL INTERESECTION WITH THE AA-1 AND AA-7 RELEASES, JULY 2 AND 4, 1992

4.2 HEATING OBSERVATIONS

For the CRRES experiments, the Arecibo heater beam was tilted slightly to illuminate the planned rocket release volume. This altered the transmission pattern of the heater array somewhat, creating a high-level sidelobe to the south, but still providing a primary lobe that was about 5° by 10° (Groves, 1993). At a heating altitude of 250 km, this corresponds to a volume 40 km north-south, by 20 km east-west (Gordon and Dobelman, 1982). For our purposes here, we have assumed that the center of this main beam at the same altitude is the nominal rocket release position of 18.8° N latitude and –66.7° west longitude.

The low cross-field thermal conductivity limits the horizontal extent of thermal effects during heating to the immediate vicinity of the heater beam. Along the magnetic field, however,

the thermal conductivity is high; elevated electron temperatures have been observed at altitudes well above and below the heating altitude (Mantas *et al.*, 1981). The altitude profile of the elevated temperatures is controlled by the collisional loss of thermal energy to ions. The presence of the thermal pressure gradient over a range of altitudes suggests that the electron density irregularities might also be present over the same range. It is not clear, however, how the strength of the irregularities might vary with altitude, a first-order assumption being that the perturbation in density varies with electron temperature. Other processes may have significant effects on the irregularity distribution, however. For example, the polarization electric fields associated with kilometer scale heating irregularities, which map up and down the magnetic field with little attenuation (Farley, 1960), might extend the irregularity distribution beyond the altitudes of elevated temperatures.

The geomagnetic field configuration at Arecibo (dip angle 48°, declination –10°) is such that a flux tube that is heated extends upward to the south and downward to the north; from the AIO, the geostationary satellite signal source is to the northwest, at an azimuth of approximately –115° and an elevation near 45°. Intermediate-scale heater-produced irregularities should cause scintillation along the signal path whenever the raypath intersects the vertically-extended heated volume. Additionally, these irregularities have a long lifetime (tens of minutes) and can convect from the heater beam if background electric fields are present, decaying with time and separation from the heated volume. Thus, interpretation of the observed spatial pattern of heater-generated structure needs to be made, considering both the propagation geometry and the background conditions.

4.2.1 July 4 Experiment

The analysis of the heater-induced scintillation data from the three rocket nights logically begins with July 4, since the aircraft trajectory on this day was such that baseline, minimal scintillation conditions can be specified. In particular, the satellite signal level received aboard the AIO depends on the pattern of its UHF satellite receiving antenna. Because that antenna is not centered directly on the top of the aircraft, there is a significant difference in gain for eastward versus westward received signals. Additionally, the racetrack pattern within which the aircraft flew prior to tracking the barium releases consisted of multiple northwestward-southeastward legs, as are shown in Figure 12, so there was a difference in received signal level that needs to be considered.

As pointed out above, the effects of heater-generated irregularities on a propagating signal are subtle. For the degree of heating obtained at Arecibo, and the frequency of the carrier used for these observations, no significant amplitude scintillation will be produced by heating, and no obvious periods of phase scintillation can be seen in the signal time series. Therefore, a signal analysis approach has been taken that uses the power spectrum of the complex received signal. This provides approximately 50 dB of dynamic range to the signal analysis, so that very subtle propagation effects can be gleaned from the data. However, care needs to be taken to accurately obtain the baseline spectra with which the heating volume data will be compared.

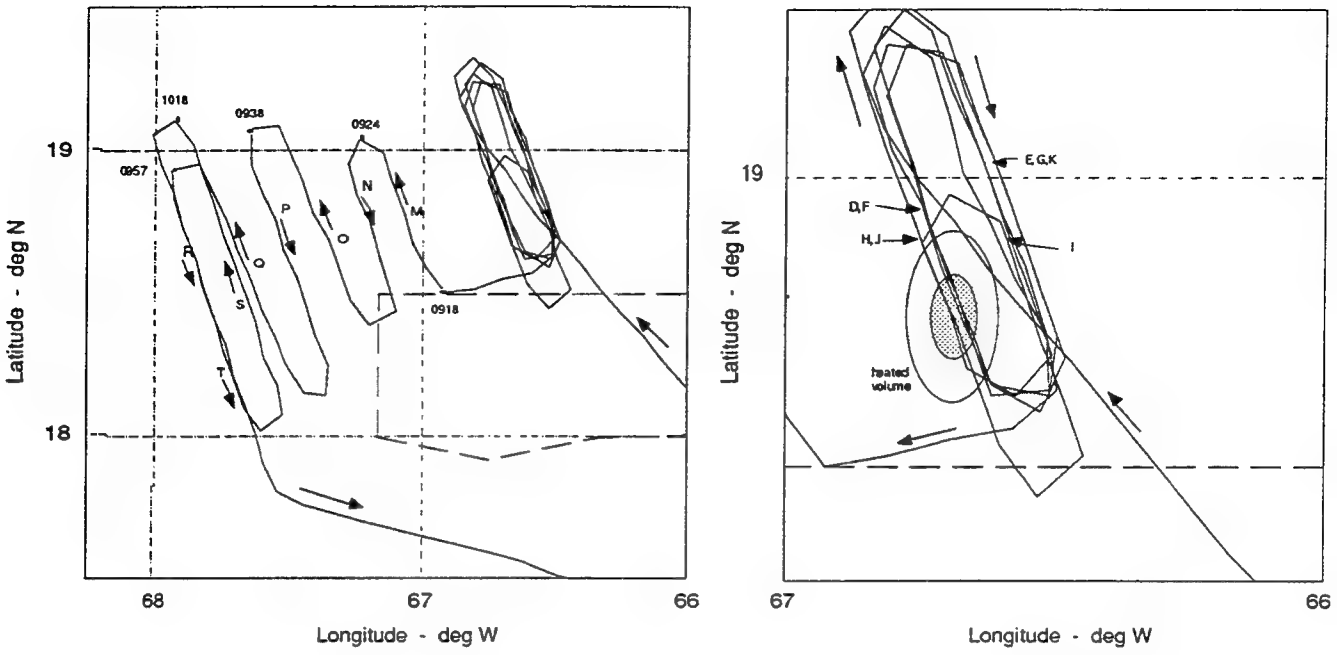

Figure 12 MAP OF THE 250 km ALTITUDE PROPAGATION PENETRATION FROM THE AIO, JULY 4, 1992

The map in Figure 12 shows the location of the ionospheric penetration point at an altitude of 250 km for the July 4 experiment. Superimposed on the map is an estimate of the nominal pattern of the main heater beam at the same altitude. It can be seen that only the northbound aircraft legs in the racetrack intercept the heater beam. Presumably, the spectra from these legs, compared to those for interspersed southbound legs to the east, should show energy contributions due to heating. Unfortunately, those spectra cannot be directly and simply compared because of the difference in received SNR between the northbound and southbound scans. However, it is possible to derive an accurate "no heating" baseline spectrum with which heating spectra can be compared using data from the combination of northbound and southbound legs collected at later times. The pattern of these later legs, which were flown in an attempt to track the cloud, is shown in the larger scale map in Figure 12. Data from legs M and N were likely contaminated by cloud intersections and could not be used, but this was not the case for the later observations. Furthermore, the farther-west legs are less likely to encounter any remnant of heater-generated structure that might have convected from the heater beam.

As the map in Figure 12 shows, the only scan through the heater beam occurs during the beginning of each northbound leg in the racetrack. On this day, the heater operated with only two transmitters. In previous Islote experiments, the use of only two transmitters broadened the main lobe of the heater beam and effectively reduced the power density by a factor of two relative to the four-antenna configuration. For this reason, the approximate extent of a beam broadened by a factor of two from the nominal pattern has also been superimposed on the map. Even with the broadened beam, only the northbound racetrack signal paths on July 4 passed through the heated volume.

Figure 13 is a comparison between the spectra from northbound legs O and Q, and those from southbound legs P and R. Each spectrum shown is the average of three or more spectra computed from data over the approximately 5-minute duration of each leg, with care taken to avoid any geometrical Doppler contamination near the turns. The bulk of the energy in the spectra is at low frequencies, and is the sidelobe power from the large, slow phase variations that result from very large-scale changes in TEC that are always present in the quiet ionosphere. These sidelobes effectively obscure any scintillation variations at frequencies below about 0.1 Hz, or about 2000 m spatial scale assuming an aircraft scan velocity of 200 m/s. The figure shows that higher SNR for the southbound legs creates an obvious and systematic difference in the spectral form, despite the fact that virtually the same undisturbed ionospheric background is being probed. These spectral forms are the baseline form against which we will compare all of the heater data.

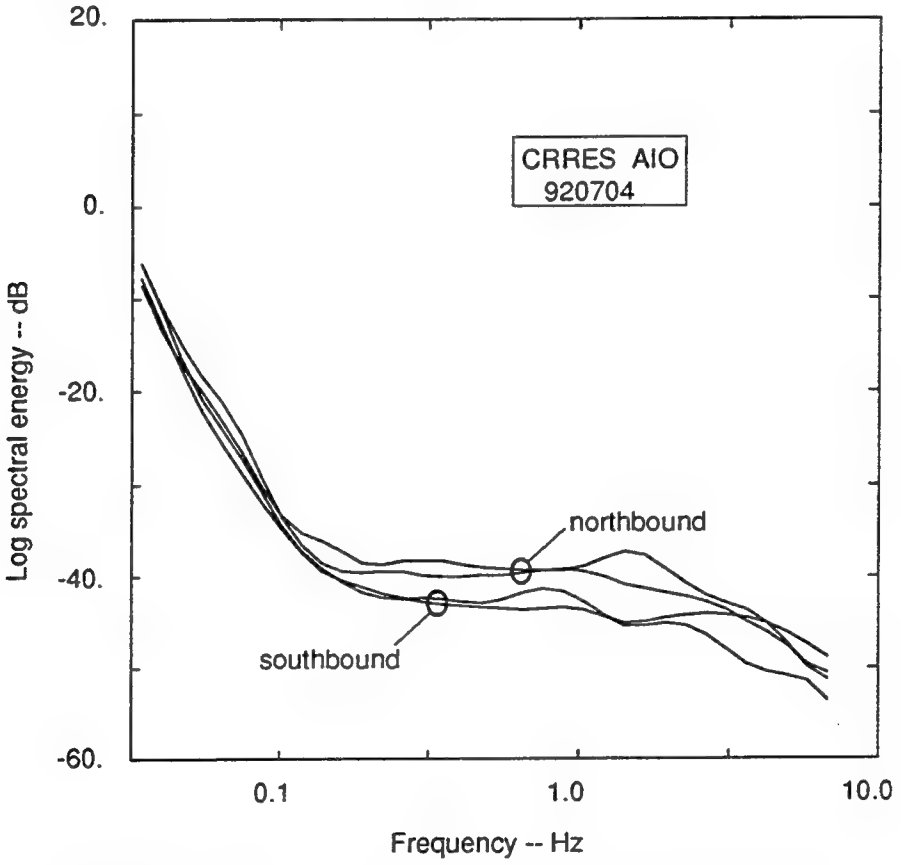

Figure 13 SPECTRAL ENERGY COMPARISON, NORTHBOUND VS SOUTHBOUND FLIGHT DIRECTION, NO-HEATING, JULY 4, 1992

During the early morning at Arecibo, the F layer peak electron density typically declines as the layer altitude drops. Profiles of electron density measured by the Arecibo radar at 0906 UT (Figure 3) show the peak of the F layer near 270 km, and a plasma frequency near 6 MHz. Data from the FAR ionosonde and Arecibo radar prior to about 0900 UT should be processed to provide more detail about the background ionosphere, but for now it is assumed that the heating was taking place near an altitude of 250 km on the F layer bottomside. The heater operated a relatively short period of time (between 0818 UT and 0835 UT) with the two transmitters each radiating 100 kW

continuous wave (CW) at 5.1 MHz. However, the heater had operated in a 5 minute on/off mode for about two hours prior to 0818 UT using the same transmitter configuration. The lifetime of the hundreds-of-meters irregularities is long enough that a long-standing volume of irregularities should have remained from that cycled heating. As has been noted, the background ionospheric drifts were very small during the period of sustained heating, so no convective transport of the structure out of the beam would be expected.

Based upon engineering information from a 1981 heating experiment using the Islote heater (Livingston, 1988), the *in situ* power density for the 2 by 100 kW mode should have been approximately 30 $\mu W/m^2$. For this power density and typical ionospheric conditions, Cragin *et al.* (1977) predict a dominant thermal self-focusing irregularity wavelength of about 900 m. Observed in data collected from the aircraft, this dominant irregularity scale would appear in the scintillation spectra near 0.2 Hz.

A comparison of the data from the north- and southbound legs of the racetrack with the baseline spectral forms are shown in Figure 14. As should be expected, the southbound race track spectra from legs E and G, away from the heater, are indistinguishable from the baseline observed at later times, well to the west. There is a significant difference, however, between the data from legs D and F that passed through the heater beam, relative to the baseline northbound spectral form. A broad enhancement of energy is observed over the frequency range from about 0.3 Hz to 5 Hz (approximate spatial scales of 600 m to 40 m). As mentioned, there is a large-scale limit to a reliable estimate of heater-induced effects that can be derived at a frequency near 0.1 Hz: at larger scales, the sidelobes of the background slow TEC variations mask any spectral enhancements.

Legs H and I within the racetrack were shortened in order to optimize the AIO position for the pending rocket launch. Data from these legs were somewhat contaminated by geometrical Doppler and are not shown. The third spectrum in Figure 14 is for flight leg J, which occurred approximately 30 minutes after heating had ceased. As might be expected, the heater-induced structure at the highest frequencies has eroded, creating a more distinct peak near 1.2 Hz, or approximately 170 m spatial scale. The estimated decay rate for this scale size (Heelis and Vickrey, 1990) is On the order of 1500 seconds, which is in good agreement with these observations.

4.2.2 July 2 Experiment

On July 2, the heater was first turned on at 0740 UT and operated until 0821 UT in a CW mode with four transmitters, each at 50 kW output power. The ionospheric background conditions were similar to those described for July 4. At 0730 UT, just prior to heating, FAR ionograms show an foF2 of about 7.3 MHz, declining to about 6.2 MHz near the end of the cycle (0742 UT). By 0856 UT, the foF2 had further declined to about 5.6 MHz. This suggests that at 5.1 MHz, the heating was taking place on the bottomside of the F layer, not too far below the altitude of peak density. From the data analyzed to date, the specific height of the F layer is not known prior to about 0900 UT, when Arecibo radar profiles show the F layer peak at an altitude near 270 km. It is safe to assume that the layer altitude was above 250 km throughout the heating cycle, although this should be verified.

Figure 15 is a map of the aircraft signal path ionospheric penetration at an altitude of 250 km for the July 2 experiment. Superimposed on the map is the nominal heater beam pattern at the same altitude for the four antenna mode. The northward legs of the racetrack each intersect the

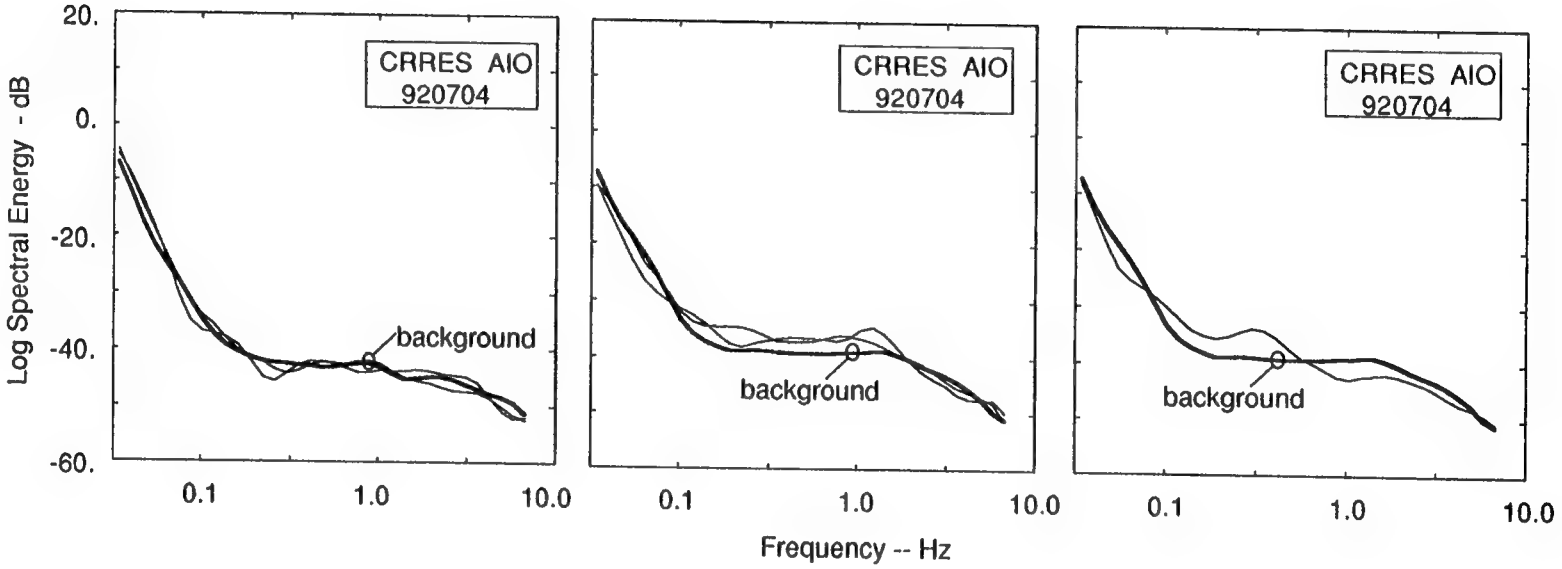

Figure 14 SPECTRAL ENERGY, SOUTHBOUND LEGS E, G WITH NO HEATING (LEFT), NORTHBOUND LEGS D, F WITH HEATING (CENTER), AND NORTHBOUND LEG J POST HEATING (RIGHT), RELATIVE TO BASELINE SPECTRA, JULY 4, 1992

heated volume and should encounter heater-generated scintillation structure. The southward legs penetrate well to the east of the heater beam. Furthermore, on this morning the F layer winds shown in Figure 1 were consistently westward at about 60 m/s and would convect any heater-generated structure only to the west.

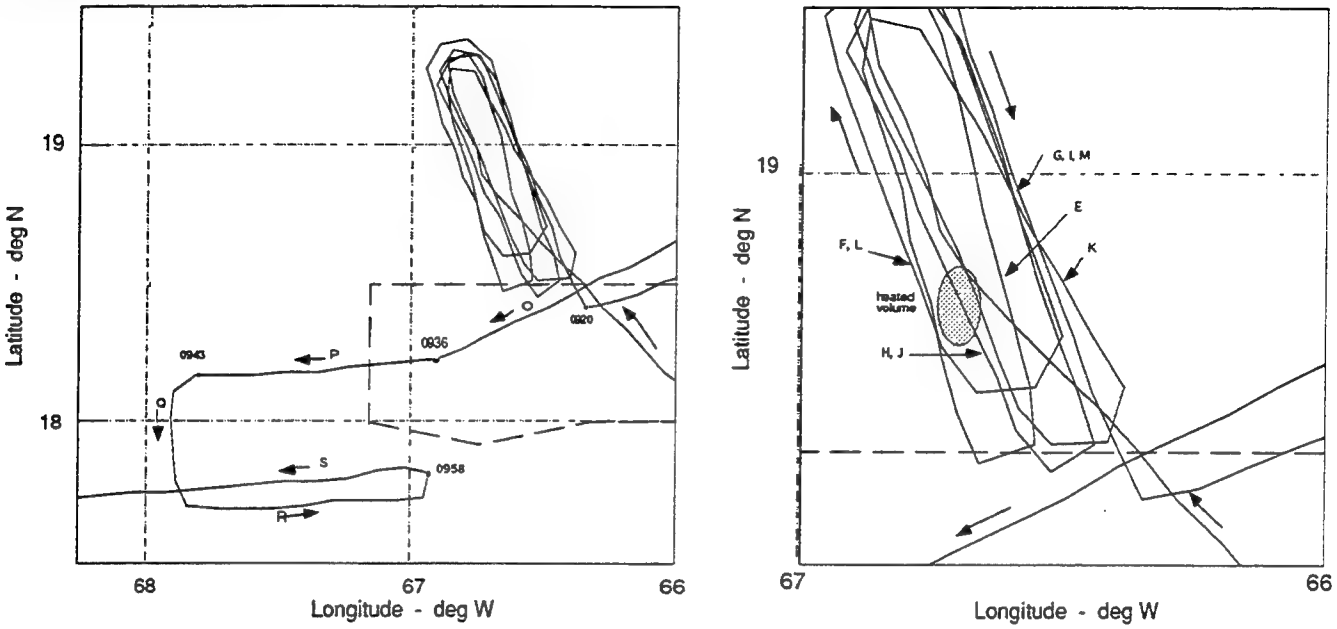

Figure 15 MAP OF THE 250 km ALTITUDE PROPAGATION PENETRATION FROM THE AIO, JULY 2, 1992

Figure 16 compares the spectra from the north- and southbound legs of the racetrack, and show the anticipated effects of heater irregularities. The spectra for legs G and I, which are well east of the heated volume, show little deviation from the baseline southward spectrum measured on July 4. Such good agreement between data measured on different days further validates the baseline measurements.

The spectra from legs D, F, and H are quite similar in shape, and are compared to the northbound baseline spectrum in Figure 16. Each of these legs passed through the heated volume during, or within a few minutes of active heating. The difference in average energy between the heater and the baseline spectrum provides a rough idea of the shorter-scale portion of the irregularity spectrum produced during the July 2 heating. The energy is greater than that seen on July 4, which might be attributable to the higher effective power density. The energy enhancement also shows a broad peak centered at a frequency of about 1.6 Hz, or a spatial scale near 130 m. The estimated power density for this mode (based upon the 1981 information) should have been about 85 $\mu W/m^2$ from which thermal self-focusing theory would predict a spatial wavelength near 670 m. Clearly, the peak observed in these data cannot be explained by that theory.

4.2.3 July 12 Experiment

The penetration path map for the AIO on July 12 is shown in Figure 17. Unfortunately, the penetration paths during the racetrack legs all passed to the east of the heated volume. As this would imply, there is little suggestion of any heater-induced structure in any of the observed scintillation data.

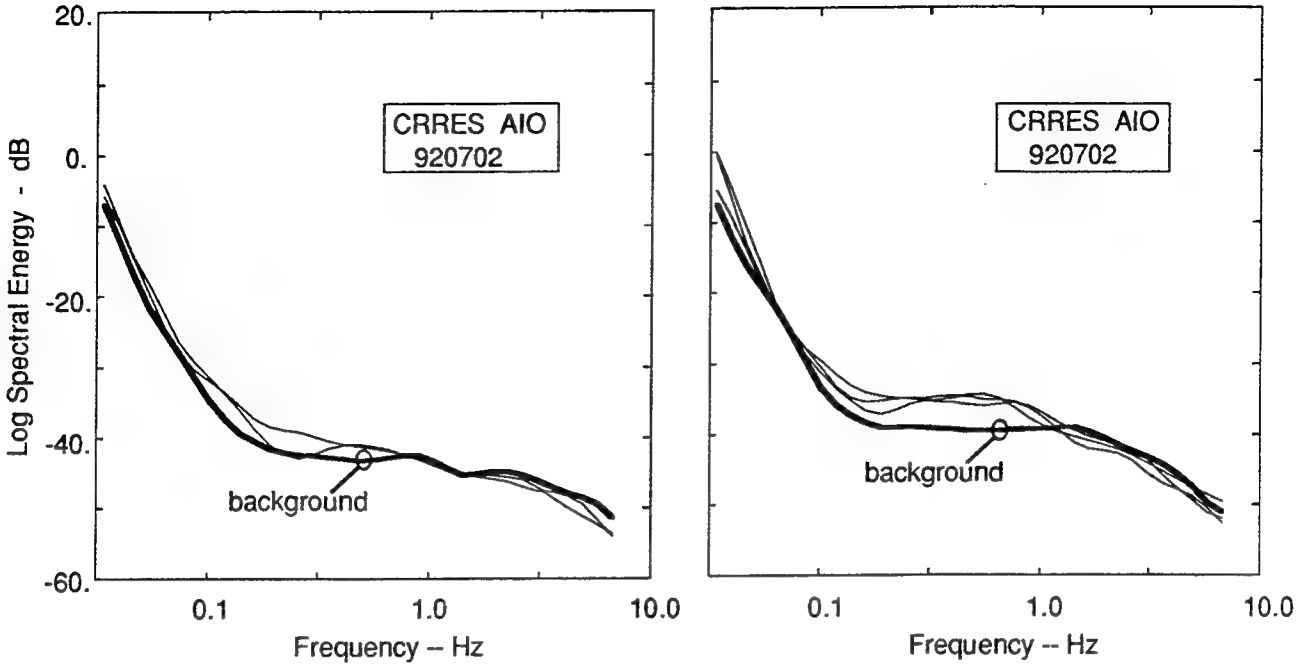

Figure 16 SPECTRAL ENERGY, SOUTHBOUND LEGS G, I WITH NO HEATING (LEFT) AND NORTHBOUND LEGS D, F, H WITH HEATING (RIGHT), RELATIVE TO BASELINE SPECTRA, JULY 2, 1994

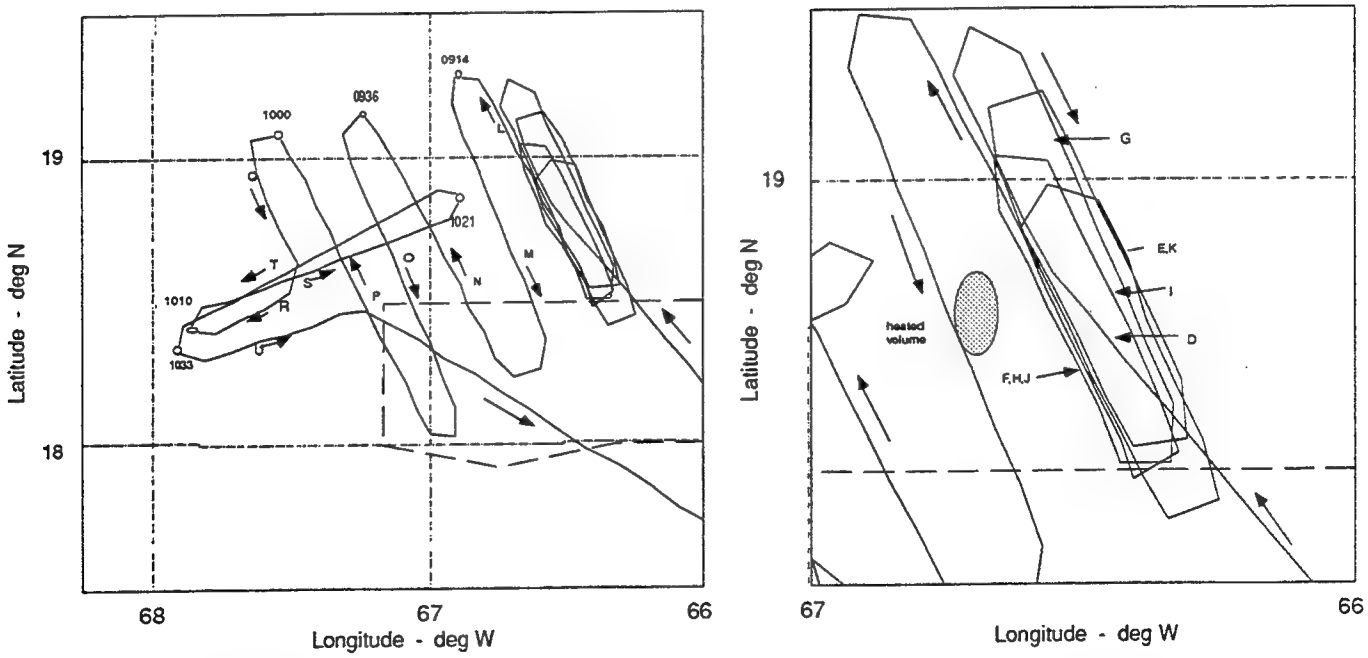

Figure 17 MAP OF THE 250 km ALTITUDE PROPAGATION PENETRATION FROM THE AIO, JULY 12, 1992

Figure 18 compares southbound legs in the racetrack (G and I) with the southbound baseline spectral form measured on July 4, and confirmed using July 2 data. The differences are negligible, as should be expected. Northbound legs F, H, and J are compared to the northbound baseline in the right panel of the figure. On average, there is no systematic difference between the spectra, although all three legs do show peaks in energy at frequencies greater than about 1.5 Hz. This could be attributed to heater-generated structure that has convected from the heater volume to the west. Some support for this idea comes from the spectrum of leg M, which passed through the heater beam at about 0918 UT, and shows a similar distinct peak of energy at a frequency near 4 Hz.

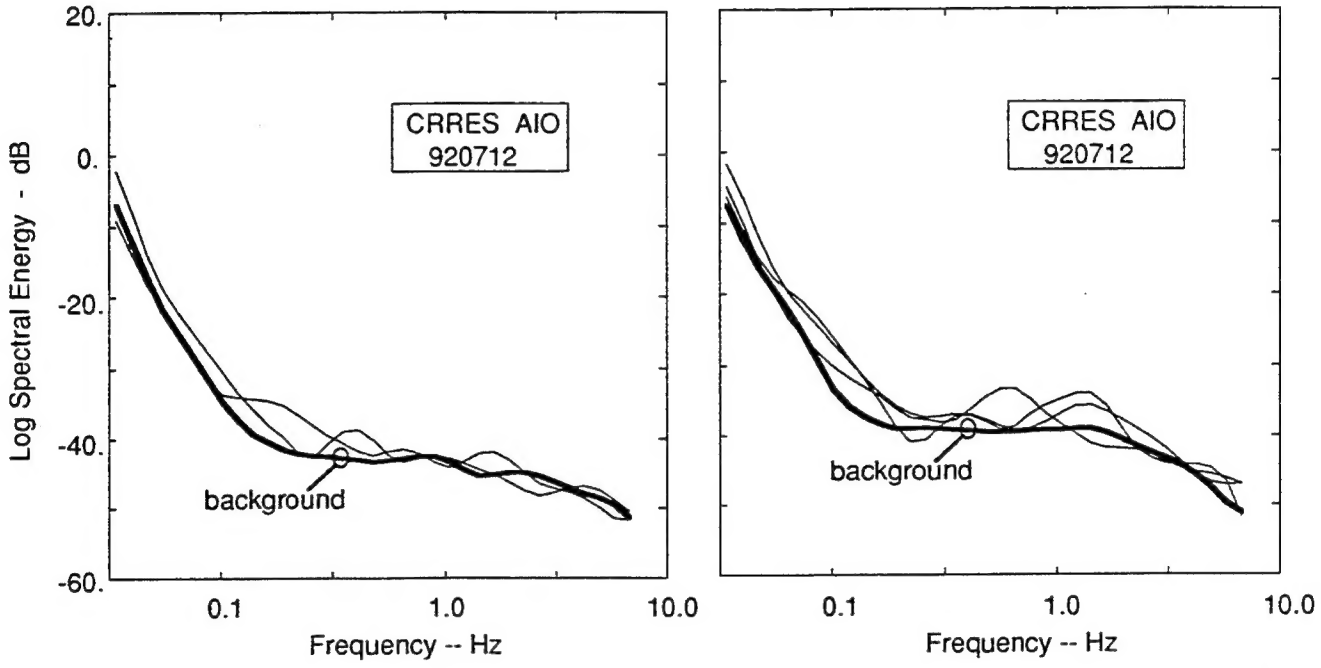

Figure 18 SPECTRAL ENERGY, SOUTHBOUND LEGS G, I WITH NO HEATING (LEFT), AND NORTHBOUND LEGS F, H, J WITH NO HEATING (RIGHT) COMPARED TO BASELINE SPECTRA, JULY 12, 1992

Any further interpretation of the July 12 scintillation data should be made in conjunction with a review of the background ionospheric conditions observed by the Arecibo radar. The heater power density for this experiment was significantly higher than on July 2 or July 4, and the heater had remained on for an extended period prior to the AIO observations. Accordingly, if the background conditions can be established, the scintillation data may provide some useful insights into the thermal self-focusing processes.

5 SUMMARY

This report has briefly outlined the early analysis of data from the CRRES Puerto Rico rocket releases and their associated heating experiments. Although the ion clouds did not striate or produce images, there is much of scientific interest in the data from the Arecibo Observatory ISR, the FAR radar, and the AIO propagation experiment. There is evidence in the ISR and FAR data of formation of velocity shear regions near the edge of the barium cloud, and more detailed analysis of the data is warranted. The ISR data also provide a unique opportunity to define, in detail, the photoionization process within the barium cloud by formally analyzing the composition of the plasma. Future heating experiments should investigate the broad enhancement of irregularities seen in the AIO scintillation data that are not explained by the traditional self-focusing theory.

6 REFERENCES

Burns, A.A. and R.C. Livingston, "RF beacon experiment results, Proceedings of the SECEDE II Final Data Review Meeting," Rome Air Development Center Report RADC TR-72-153, vol. 2, 1972. **ADB901004L**

Cragin, B.L., J.A. Fejer, and E. Leer, "Generation of artificial spread-F by a collisionally coupled purely growing parametric instability," *Rad. Sci.*, 12, 273, 1977.

Djuth, F., M.P Sulzer, J.H. Elder, and K.M. Groves, "The CRRES AA-2 release: HF wave-plasma interactions in a dense Ba^+ cloud," submitted for publication, *J. Geophys. Res.*, 1993.

Drake, J.F., M. Mulbrandon, and J.D. Huba, "Three-dimensional equilibrium and stability of ionospheric plasma clouds," Naval Research Laboratory Memorandum Report 6436, 1989.

Farley, D.T., "A theory of electrostatic fields in the ionosphere at nonpolar geomagnetic latitudes," *J . Geophys. Res.*, 65, 869, 1960.

Gagnon, R. and J.M. Lansinger, "An approximate method for computing diffraction patterns caused by ionospheric irregularities," *Rad. Sci.*, 68D, 737, 1964.

Gordon, W.E. and J.A. Dobelman, "Comparison of measured and calculated antenna patterns for the Islote heater," report, Rice University, Houston, Texas, 1982.

Groves, K.M., personal communication, 1993.

Heelis, R.A. and J.F. Vickrey, "Magnetic field-aligned coupling effects on ionospheric plasma structure," *J. Geophys. Res.*, 95, 7995, 1990.

Linson, L.M., "Status of theoretical understanding of barium ion cloud phenomenology," Proceedings of the SECEDE II Final Data Review Meeting, Rome Air Development Center Report RADC TR-72-153, vol. 2, 1972. **ADB901004L**

Livingston, R.C., "Phase scintillation measurements during ionospheric modification at Arecibo," Technical report contract F19628-84-K-0019, SRI International, Menlo Park, California, 1988.

Mantas, G.P., H.C. Carlson, and C.H. LaHoz, "Thermal response of the F region ionosphere in artificial modification experiments by HF radio waves," *J. Geophys. Res.*, 86, 561, 1981.

Rino, C.L., "A power law phase screen model for ionospheric scintillation studies, 1. weak scatter," *Rad. Sci.*, 14, 1135, 1979.

Shen, J.S., W.E. Swartz, D.T. Farley, and R.M. Harper, "Ionization layers in the nighttime E region valley above Arecibo," J. *Geophys. Res.*, 81, 5517, 1976.

St.-Germain, R.L., E.M. Allen, and G.D. Thome, "HF phased array observations in the ion clouds during SEDEDE II," Proceedings of the SECEDE II Final Data Review Meeting, Rome Air Development Center Report RADC TR-72-153, vol. 2, 1972. **ADB901004L**

Sulzer, M.P., "A phase modulation technique for a sevenfold statistical improvement in incoherent scatter data-taking," *Rad. Sci.*, 21, 737, 1986.

Tsunoda, R.T., "Incoherent scatter events for event Spruce," Proceedings of the SECEDE II Final Data Review Meeting, Rome Air Development Center Report RADC TR-72-153, vol. 2, 1972. **ADB901004L**

Tsunoda, R.T., J. Buonocore, R.C. Livingston and A. McKinley, "The frequency-agile radar: A multi-functional approach to remote sensing of the ionosphere," SRI Technical Report, project 3982, 1993.

Waterman, P.C., G. Meltz, and N.M. Tomljanovich, "The effect of barium ion cloud distortion on HF backscattering," Proceedings of the SECEDE II Final Data Review Meeting, Rome Air Development Center Report RADC TR-72-153, vol. 2, 1972. **ADB901004L**

Zambre, Y., "A generalized program for fitting incoherent scatter autocorrelation functions," SRI Technical Report, project 7117, 1993.